Lithos 111 (2009) 125–141

Contents lists available at ScienceDirect

Lithos

journal homepage: www.elsevier.com/locate/lithos

Layered granitoids: Interaction between continental crust recycling processes and mantle-derived magmatism
Examples from the Évora Massif (Ossa–Morena Zone, southwest Iberia, Portugal)

Patrícia Moita [a,*], José F. Santos [b], M. Francisco Pereira [a]

[a] Centro de Geofísica de Évora/Departamento de Geociências da Universidade de Évora, Apartado 94, 7002-554, Évora, Portugal
[b] Geobiotec, Departamento de Geociências da Universidade de Aveiro, Campus de Santiago, 3810-003 Aveiro, Portugal

ARTICLE INFO

Article history:
Received 7 March 2008
Accepted 28 February 2009
Available online 12 March 2009

Keywords:
Layered granitoids
Calc-alkaline magmas
Crustal anatexis
Fractional crystallization

ABSTRACT

In this paper, field, petrographic, mineralogical, geochemical and isotopic (Rb–Sr and Sm–Nd) information from three areas within the Évora Massif (Iberian Variscan Orogen) is presented and discussed aiming at to unravel the relationships between granitoids and units mapped as migmatites and also to evaluate the interplay between mantle and crustal derived magmas.

One of the areas – Almansor – displays a well-developed compositional layering (concordant with the regional Variscan structure) which was considered, in previous works, as an alternation of leucosome and melanosome. In this study, the layering is described as intercalation of diatexites, weakly foliated granitoids and trondhjemitic veins. Diatexites have characteristics of crustal melts plus restitic material and, according to geochemical and isotopic evidence, result from anatexis of Ediacaran metasediments. Weakly foliated granitoids and trondhjemitic veins from Almansor have calc-alkaline signatures and may be related to each other by crystal fractionation processes; however, the mixing between mafic (mantle-derived) and felsic (diatexitic melt) magmas revealed by the isotopic data may also explain their genesis.

In the Alto de São Bento area, several igneous lithologies (tonalites, granodiorites, porphyritic granites and leucogranites) are present and show typical isotropic igneous textures. Despite structural and textural differences, geochemical data support, for most rocks, an origin from the same calk-alkaline suite, also present at Almansor. The Alto de São Bento leucogranites have an isotopic signature that, although different from that obtained in the Almansor diatexites, is still compatible with an origin involving melting of Ediacaran metasediments; compositions, with very low contents of usually incompatible elements, flat normalized REE patterns and strong negative Eu anomalies, suggest that the anatectic melt has undergone crystal fractionation processes before reaching the composition of the leucogranite magma.

The Almansor outcrop is then interpreted as the remnants of a shear zone that operated as a pathway for melts that moved upward through the crust providing the locus for differentiation and mingling/mixing of magmas, whilst Alto de São Bento would correspond to the zone, at a higher crustal level, where magmas were trapped and forced to spread horizontally.

At Valverde (the third area) foliated and non-foliated granitoids are spatially related and field criteria links these rocks to metamorphic protolith and anatectic melt, respectively. However, petrographic, geochemical and isotopic information shows that they all are compositionally identical trondhjemites with no evidence of metamorphic fabric. In the foliated rocks, mesoscopic features are interpreted as resulting from melt segregation structures formed in a crystallizing mush. In contrast to the previous areas, the Valverde trondhjemites probably do not belong to the main calc-alkaline plutonic suite of the Évora Massif, since they have a distinct Sr and Nd isotope signature.

1. Introduction

Geotectonic units from high-grade metamorphic terrains affected by major orogenic events present complex cartographic patterns. These result from the great variety of lithotypes, the superposition of several phases of deformation and the presence of relics of processes in the transition of metamorphic and magmatic domains (Mehnert, 1968; Passchier et al., 1990; Milord and Sawyer, 2003).

In many units, the distinction between migmatites and layered granitoids is often difficult to establish, particularly if intrusion of thin magmatic veins and/or mingling of different magmas occurred in the same crustal levels where migmatites are expected (Milord et al.,

* Corresponding author. Tel.: +351 266745301; fax: +351 266745397.
E-mail address: pmoita@uevora.pt (P. Moita).

0024-4937/$ – see front matter © 2009 Elsevier B.V. All rights reserved.
doi:10.1016/j.lithos.2009.02.009

2001; Pereira and Lúcio, 2007). As a consequence, it is not uncommon, according to Pawley et al. (2002), that some layered granitoids are mapped as migmatitic gneisses, despite the fact that they do not fit the most common definitions of migmatites. Although the migmatites have been the matter of many geological discussions, they can be considered, in a modern view, as heterogeneous rocks comprising different parts, one of which (neosome) must have formed by partial melting; neosome is typically (but not always) divided into a light coloured quartz-feldspathic portion (leucosome), displaying magmatic textural features, and a dark coloured ferromagnesian-rich fraction (melanosome), representing the residuum (Mehnert, 1968; Brown, 1973; Sawyer, 2008).

Some types of layering may be caused by metamorphic/subsolidus processes, such as chemical segregation of a heterogeneous protolith due to differential mobility of elements (Robin, 1979; Sawyer and Barnes, 1988; Barbey et al., 1989) and transposition of originally oblique veins during intense shortening (Myers, 1978). Nevertheless, there are also alternative magmatic models, which were argued to explain compositional layering such as injection of magma into low pressure sinks whose orientation is parallel to a pre-existing foliation (Lucas and St-Onge, 1995) and injection of magmas into an active shear zone (Pawley et al., 2002).

Besides layering, the other mesoscopic features typically found in outcrops of migmatitic units are melt segregation structures (e.g. Mehnert, 1968; Brown, 1994; Sawyer, 2001). Although these structures are scarcely referred for granitic rocks, some authors noted their existence (Sawyer, 2000; Weinberg et al., 2001; Weinberg, 2006). According to Weinberg (2006), the recognition of rare or subtle melt segregation features in plutonic rocks may provide key information about fractionation within granitic magma chambers.

In this paper, field, petrographic, mineralogical, geochemical and isotopic (Rb-Sr and Sm-Nd) information from critical areas located in central Portugal (Évora Massif) will be presented and discussed aiming at to unravel the relationships between granitoids and units mapped as migmatites. In fact, some outcrops with a "migmatitic look" may rather be the result of interpenetration and/or segregation of melts with different compositions in a dominantly magmatic environment. Additionally, those areas are also expected to demonstrate the interplay between magmas of both crustal and mantle provenance, through processes of anatexis and several types of magmatic differentiation.

2. Geological setting

The Évora Massif (Carvalhosa, 1983; Pereira et al., 2007) is located in the southwest of Iberia (Fig. 1A) and corresponds to a geological unit within the Ossa–Morena Zone (one of the major divisions of the Iberian Variscan Orogen) outcropping around and between the towns of Montemor-o-Novo and Évora (Fig. 1B). This domain is mainly composed of Ediacaran, Cambrian and Ordovician country rocks (Carvalhosa, 1983; Oliveira et al., 1991; Cordani et al., 2006; Chichorro et al., 2008), affected by medium and high-grade metamorphism (Carvalhosa and Zbyszewski, 1994; Chichorro, 2006) coeval with the emplacement of large mafic to felsic intrusive bodies (Moita, 2007).

The Ediacaran–Cambrian(–Ordovician?) meta-sedimentary and meta-igneous rocks were mainly affected by Variscan metamorphism with a clockwise P-T-t path that attained 750 °C and 6 kbar (Chichorro, 2006). A syn-metamorphic pervasive sub-vertical foliation striking N310° is the most conspicuous structural feature. The continuous sinistral shearing responsible for strong mylonitization associated with folds with axes subparallel to a subhorizontal- to moderately dipping stretching lineation striking N300°–310° defines a main tectonic transport parallel to the orogen (transcurrent movement, Pereira et al., 2007).

In the western end of the Évora Massif, the Lower Palaeozoic rocks are unconformably overlain by Upper Devonian and Lower Carboniferous terrigenous sediments and basaltic to andesitic volcanic rocks, only very weakly metamorphosed, that constitute the Cabrela syncline (Ribeiro, 1983; Carvalhosa and Zbyszewski, 1994; Chichorro, 2006). Therefore, the tectonic evolution of the Évora Massif was very complex and included intra-orogenic extension.

As a whole, the Évora Massif has a dome-like structure bounded by major detachments and presenting a core of high-grade metamorphic rocks: the Évora high-grade metamorphic terrain (EHMT), as defined by Pereira et al. (2003). The EHMT comprises a structurally complex assemblage of variably sheared migmatites and gneisses intruded by Variscan plutonic rocks whose compositions range from gabbros to granites, being mainly represented by tonalites and granodiorites (Moita et al., 2005a).

3. Field relations, sample location and petrography

Three areas within EHMT, considering the goals of this work and the need for good exposure, were selected for this study (Fig. 1B): (i) the Almansor area, located near Montemor-o-Novo, where variably sheared diatexites (probably derived from Ediacaran metasediments) and granitoids of principally tonalitic to granodioritic composition are intercalated with each other, defining a banded structure that can be observed in a subhorizontal exposure along a major stream; (ii) the Valverde area (~10 km SW of Évora), with outcrops of gneisses (with Lower Palaeozoic protoliths) and granitoids along a stream; (iii) the Alto de São Bento area, corresponding to a topographic elevation in the western limit of the town of Évora, where different types of granitoid rocks coexist, with particularly good exposures in the floor and walls of a quarry.

3.1. Almansor area

The outcrop studied along the Almansor stream (Fig. 2) displays a well-developed compositional layering which had been previously described as an alternation of leucosome and melanosome in a migmatite (Carvalhosa and Zbyszewski, 1994; Pereira and Silva, 2002). The layering in this exposure has a general orientation of N290° to N300°, concordant with the regional Variscan structure, and corresponds to the intercalation of (i) diatexites, (ii) weakly foliated granitoids and (iii) trondhjemitic veins. Although irregularly shaped, the contacts between the different rocks are dominantly sharp. Evidence of sinistral shear deformation, affecting either the layering or the positions and shapes of restites and enclaves, is commonly observed in the Almansor outcrop. It should be remarked that the term "diatexite" is used in this work to designate a rock with two principal characteristics (Brown, 1994; Sawyer, 1996; Sheppard et al., 2003; Sawyer, 2008): (i) it is mainly composed of neosome representing a great fraction of melt and (ii) in the neosome, pre-anatectic structures were erased and substituted by syn-anatectic flow structures or isotropic arrangements of the mineral grains. Therefore, despite often considered as a precise category of migmatites, diatexites display compositional and structural/textural features transitional to those found in typical granitoid lithologies.

The diatexites form orange or grey coloured bands whose widths vary from several centimetres to few metres (Fig. 2A,B). At mesoscopic scale, they show a distinct anisotropy, defined by the preferred orientation of biotite and of elongated dark bodies. The latter are small bodies that do not exceed 20 cm in length, have sigmoidal shapes with sharp edges (sometimes surrounded by thin felsic haloes) and display a strongly planar fabric. Their dark colour reflects the overwhelming modal dominance of biotite, with minor quartz and, sometimes, cordierite; the strong ferromagnesian composition of these bodies lead us to interpret them as restites rather than paleosomes. Several types of centimetric to metric enclaves of metamorphic origin (amphibolite, metachert, paragneiss) occur within diatexites. Generally, the shapes of enclaves are elongated along the foliation of the

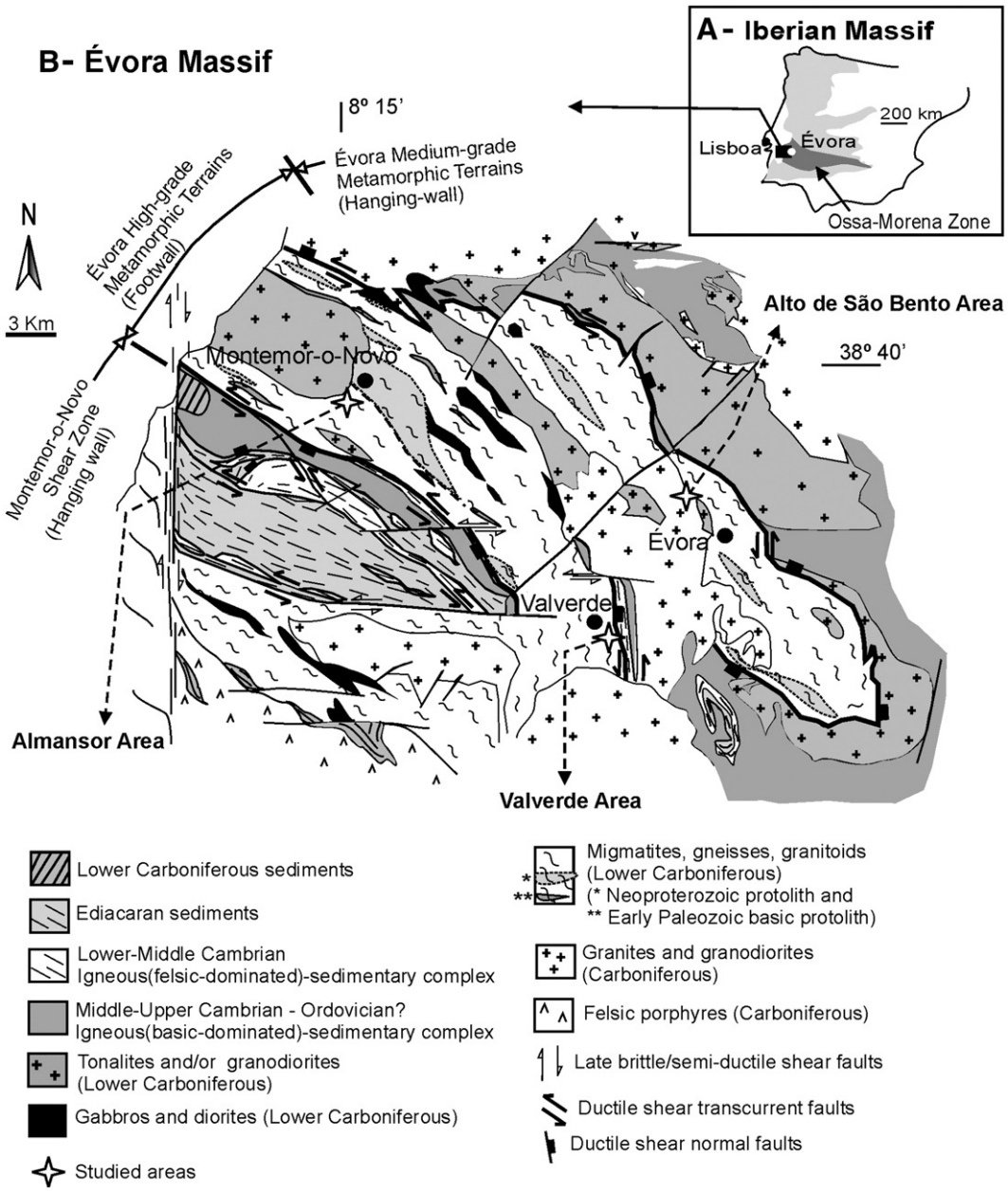

Fig. 1. (A) Localization of Ossa–Morena Zone within Iberian Massif; (B) Geological map of Évora Massif (modified from Carvalhosa and Zbyszewski, 1994) with major subdivision by Pereira et al. (2003).

planar anisotropy; some contain indicators of kinematic shear sense which indicate sinistral movement.

The modal compositions of diatexites (Fig. 3A), excluding the enclosed mesoscopic restitic bodies, overlap the fields of monzogranites and quartz-monzonites: K-feldspar (perthitic microcline) and plagioclase (An_{10-20}) are always amongst the dominant mineral phases (20% to 40%, each), whereas the proportion of quartz varies from 10 to 25%. Biotite (with Fe# from 0.3 to 0.5) is the main mafic mineral and ranges from 5% to 15%, increasing from monzogranite to quartz-monzonite compositions. Accessory zircon and secondary muscovite were also identified in all diatexite samples. In contrast, pinitized cordierite was found only in quartz-monzonitic diatexite.

Microtextural study of thin sections of diatexites revealed a much weaker planar anisotropy than expected from the field characteristics. In addition, the individual mineral grains, including oriented biotite crystals, are mostly undeformed.

The weakly foliated granitoids occur as bands (Fig. 2A), usually thicker than the diatexite layers, with a less obvious anisotropy (conferred by mineral preferred orientation) and different modal composition. These granitoids enclose some randomly oriented metamorphic (essentially felsic gneisses) and igneous (tonalites) enclaves and are locally crosscut by centimetric felsic dykes subparallel to the layering main orientation.

The modal composition of the weakly foliated granitoids is transitional between tonalite and granodiorite, showing dominance of plagioclase (~50%; An_{20-35}) and quartz (~30%), and minor microcline (~10%). Biotite (Fe#: 0.3–0.45) occurs in modal amounts ranging from 5 to 15%, whereas apatite and zircon occur as accessory minerals. Microtexture of these rocks is essentially hypidiomorphic (Fig. 3B) and the planar anisotropy, at microscopic scale, is not easily noticed. Plagioclase is subhedral, commonly showing either continuous or discontinuous concentric zoning. Biotite crystals are generally interstitial; there are scattered monomineralic aggregates (2–3 mm) of parallel oriented biotite grains, suggesting the preservation of metamorphic domains with lepidoblastic texture. Quartz and K-feldspar are typically interstitial phases.

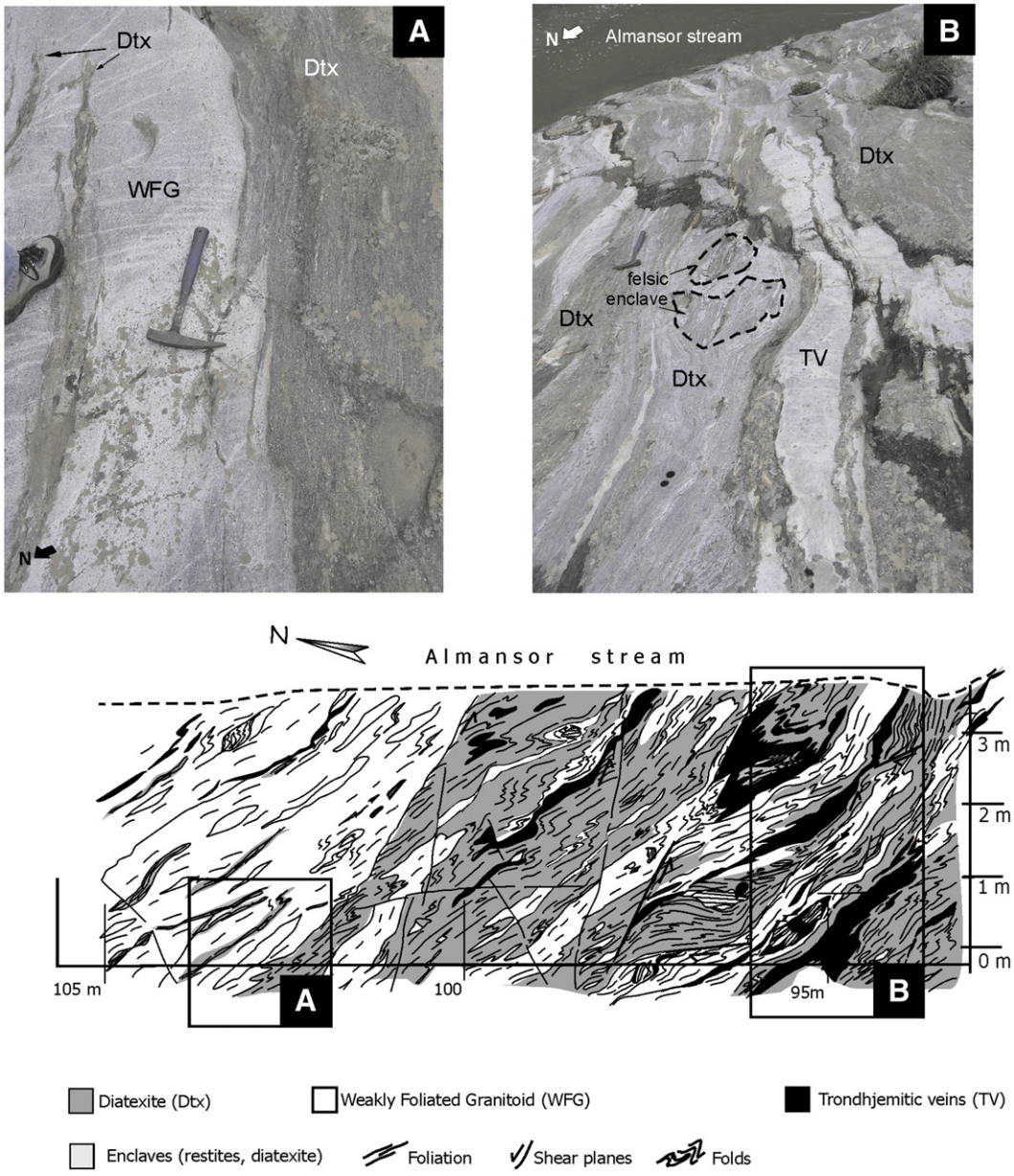

Fig. 2. Field relations of three main lithological groups observed at Almansor stream area. Photographs show relations between: (A) diatexites (Dtx) and weakly foliated granitoid (WFG); (B) diatexites and trondhjemitic veins (TV).

The designation "trondhjemitic veins" is here used to refer thin (3-30 cm wide) white-coloured veins, found within either the diatexites (Fig. 2B) or the weakly foliated granitoids. Although most commonly the veins are oriented parallel to, or at a small angle with the foliation of the host lithology, they do not show textural anisotropy. According to their composition, these rocks are classified as trondhjemites: mafic minerals are very scarce (usually less than 1%, and mainly represented by biotite) and plagioclase (~50%; An_{18-25}) and quartz (40–50%) are the major mineral phases. Microcline is the third phase in abundance, but its proportion is below 5%. Texture is granular hypidiomorphic to allotriomorphic (Fig. 3C), with subhedral plagioclase crystals, commonly displaying concentric zoning, and anhedral quartz grains.

Despite the differences in structural features at the mesoscopic scale, the main lithologies (diatexites, weakly foliated granitoids and trondhjemitic veins) of the Almansor outcrop share some important microtextural/microstrutural characteristics. Firstly, at the microscopic scale there is no penetrative tectonic foliation in these lithologies. Secondly, the commonest manifestation of subsolidus deformation are bent twins in plagioclase, and undulose extinction and subgranulation in quartz; in places, undulose extinction is also found in sheet silicates. These features are usually related to incipient deformation at low temperatures (~400 °C; Passchier and Trouw, 1998) and do not necessarily require a tectonic stress (Vernon, 2000).

Therefore, in general, diatexites, weakly foliated granitoids and trondhjemitic veins have igneous textures. The preferred orientation displayed by diatexites and weakly foliated granitoids is marked by plagioclase and biotite which are individually undeformed or just slightly deformed. These observations may be explained by mechanisms of magmatic flow, during which it is possible for rotation of crystals (acting as rigid bodies) to occur without significant mutual interference that could cause plastic deformation (Shelley, 1993; Vernon, 2000).

However, as previously referred, not only shearing structures are evident in the Almansor outcrop, but also the dominant strike of layering and planar anisotropy agrees with the general Variscan tectonic orientation in this region. Therefore, the melts represented by

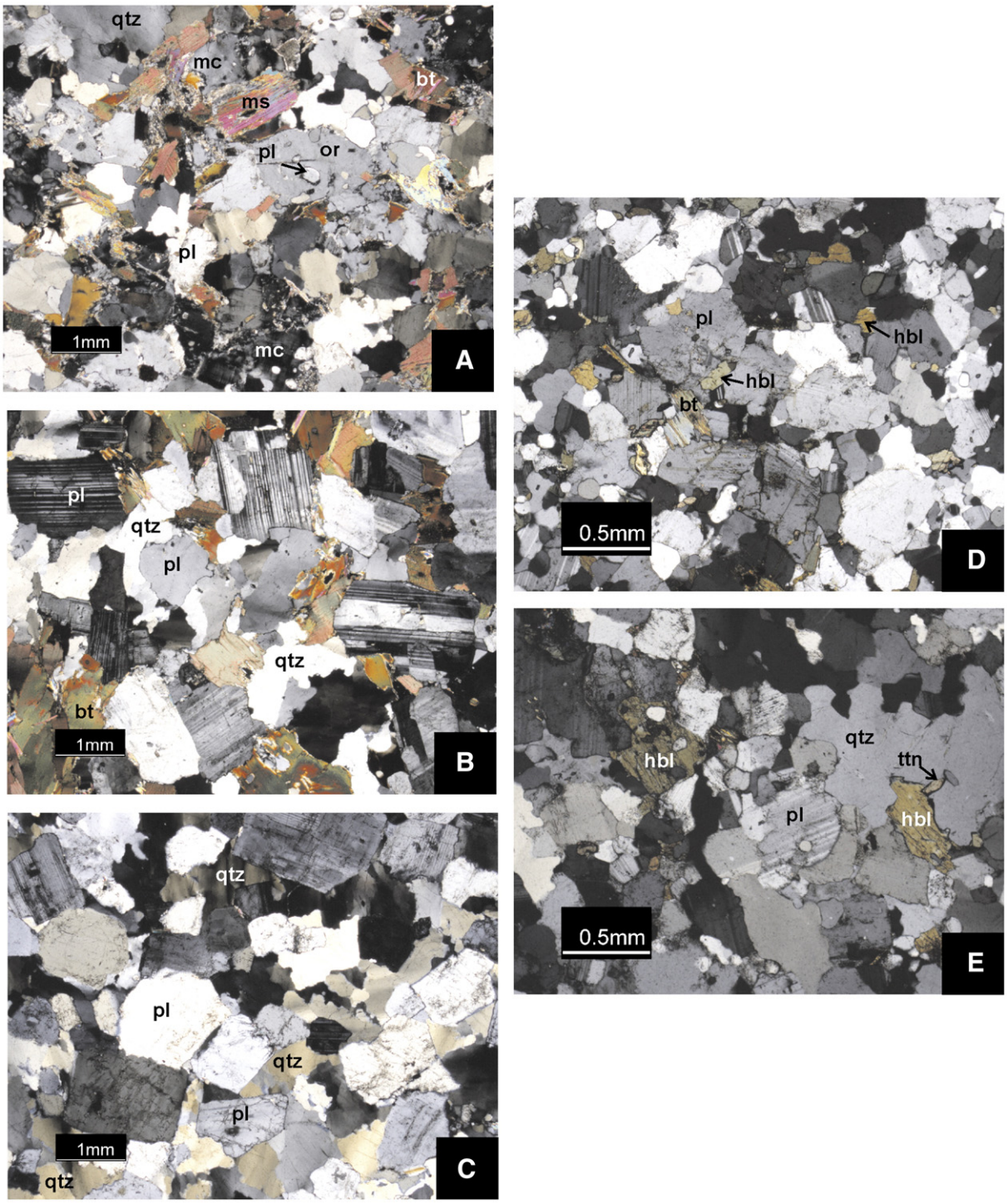

Fig. 3. Photomicrographs showing general textural aspects from Almansor: (A) diatexites, (B) weakly foliated granitoids, (C) trondhjemitic veins and from Valverde: (D) Foliated granitoids, (E) Non-foliated granitoids. Abbreviations (Kretz, 1983): bt — biotite, hbl — hornblende, mc — microcline, ms — muscovite, or-orthoclase, pl — plagioclase, qtz-quartz, ttn — titanite.

the described lithologies are interpreted to have undergone emplacement and cooling during shearing.

3.2. Valverde area

In the Valverde area (Fig. 4), it is possible to recognize, along 500 m and from E to W the following lithological sequence (Pereira et al., 2006a): micaschists, amphibolites, micaschists intercalated with amphibolites, felsic gneisses and, finally, a "migmatitic domain" with internal structures whose significance will be discussed below. Despite the strong deformation, Pereira et al. (2006a,b) claim that the described sequence probably represents in this area the regional stratigraphic column from Série Negra (Ediacaran) micaschists to Cambrian felsic gneisses (Carvalhosa et al., 1969; Chichorro, 2006).

The outcrop studied lies in the "migmatitic domain" whose main feature is the existence of a felsic rock with an evident mesoscopic subvertical planar anisotropy (striking N360-350°) – foliated granitoid – enclosing some small pods and veins also of felsic composition (Fig. 4) but showing no structural/textural anisotropy — non-foliated granitoid. Another dissimilarity noticed from the observations of the

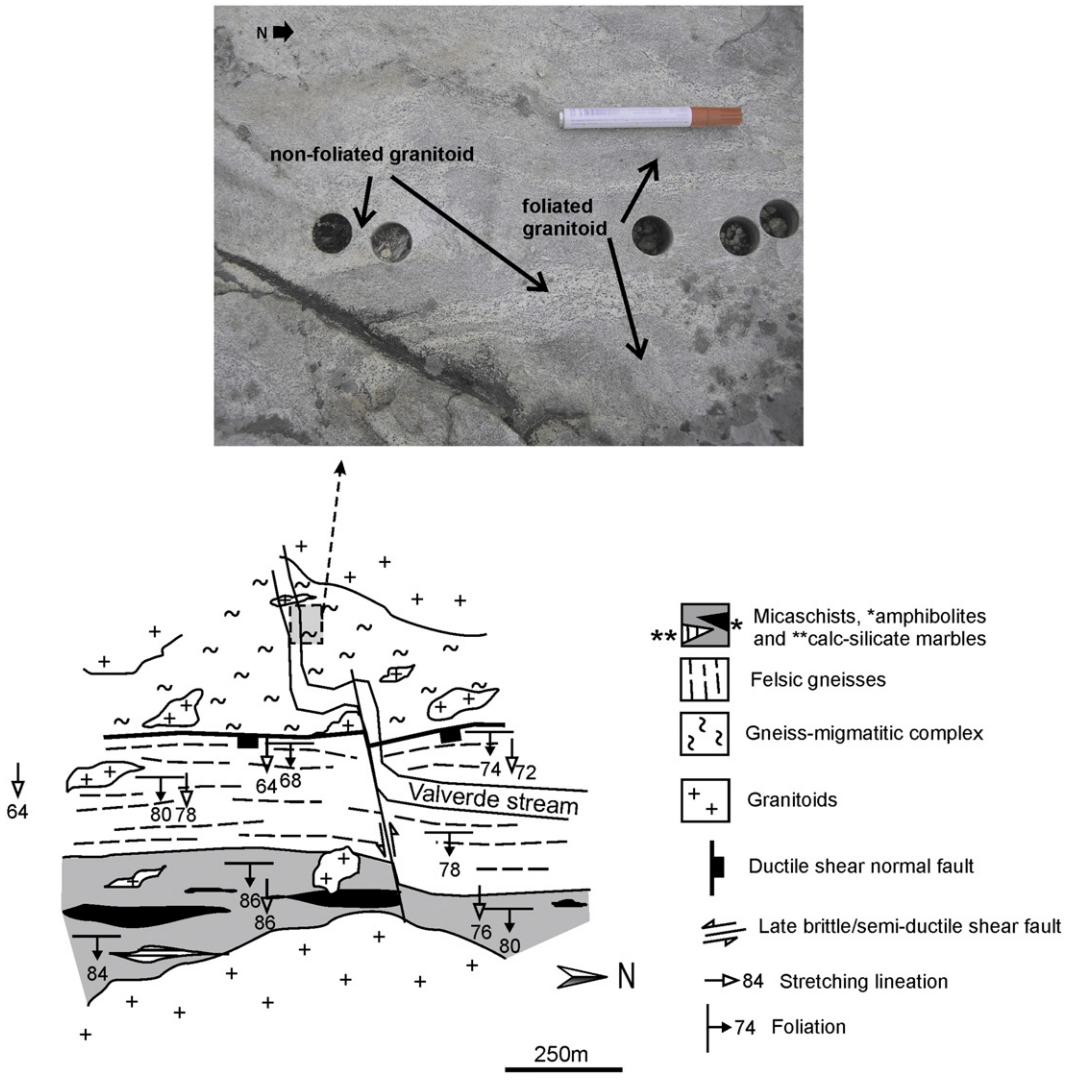

Fig. 4. Simplified geological map of the Valverde area. Photograph shows the relationship between foliated and non-foliated granitoids.

mesoscopic scale is the coarser appearance of mineral grains in the pods and veins when compared to the foliated granitoid.

However, the strong differences between foliated and non-foliated granitoids that could be anticipated from field observations were not confirmed by thin section study. In fact, the textures and modal compositions are very similar between the two types of granitoid (Fig. 3D and E) since the foliated textures become undetectable. They both exhibit a fine-grained allotriomorphic texture and have a trondhjemitic modal composition in which plagioclase (An_{5-10}) and quartz dominate and low amounts of alkali-feldspar (<5%) occur. Mafic minerals do not exceed 10% modal abundance and are represented mainly by amphibole (dominantly iron-rich hornblende with Mg#~0.4) and lesser amounts of chloritized biotite. Titanite, zircon, apatite and oxides were identified as accessory phases. The coarser aspect of the non-foliated granitoids is due to the occurrence of amphibole aggregates in the pods and veins.

3.3. Alto de São Bento area

Near the city of Évora, the Alto de São Bento quarry allows the observation of several types of granitoid rocks which previous workers (e.g. Carvalhosa et al., 1969) considered as representative of the late-tectonic intrusions. The quarry is dominated by a two-mica leucogranite, intruded by sub-horizontal sills, which can reach 5–6 m thickness, of porphyritic granite with mafic microgranular enclaves (Ribeiro, 2006). There are small and limited occurrences of granodioritic and tonalitic rocks (see below). Pegmatitic and aplitic dykes, that cross-cut the former granitoid facies, are also abundant, but they are not the focus of study.

The two-mica leucogranite is a medium-grained rock with granular allotriomorphic to hypidiomorphic texture. Its modal composition can be described as an assemblage of 35–40% quartz, 25–30% K-feldspar, 30–35% plagioclase (An_{8-10}), 5–10% muscovite and 1–2% biotite (with Fe#~0.9). Tourmaline and zircon are the principal accessory phases. Within the two-mica leucogranite it is possible to observe two tonalitic bodies, displaying a vertical magmatic layering; they probably correspond to sub-vertical intrusions. The main minerals in these bodies are quartz (20–30%), plagioclase (40–50%; An_{30-40}), K-feldspar (10–15%) and mafic minerals (15–20%; biotite with Fe#~0.6 and/or hornblende with Fe#~0.5); the accessory phases are zircon, apatite and allanite.

The porphyritic granites contain euhedral to subhedral feldspar (plagioclase and K-feldspar). Phenocrysts of K-feldspar, that may reach several centimetres in length, are surrounded by a groundmass with a grain size of 2–3 mm in which subhedral crystals are dominant. The modal composition is: 30–35% plagioclase (An_{18-28}); 20–25% K-feldspar; 30–35% quartz and 5% biotite (Fe#~0.62). Muscovite, zircon, apatite and allanite are rare accessory phases. These granites contain mafic microgranular enclaves that have a tonalitic composition: 60% plagioclase (An_{20-30}), 20% quartz and 10–15% biotite (Fe#~0.6) and

5% K-feldspar. Zircon and apatite are rare accessory phases. In the enclaves, plagioclase grains with compositions between An_{28} and An_{30} typically show subhedral cores and xenomorphic rims.

Finally, the least abundant lithotype in Alto de São Bento quarry is a medium-grained granodiorite which has a strong alignment of mafic minerals observed at mesoscopic scale. Grain shapes are typically xenomorphic. The modal composition of granodiorite is: 30–35% quartz, 20–25% K-feldspar, 40–45% plagioclase (An_{20-30}) and 10% biotite (Fe#~0.55). Apatite, allanite and zircon are rare accessory phases. The plagioclase crystals exhibit normal concentric zoning, either continuous or discontinuous.

4. Whole-rock geochemistry

In this study, whole rock compositions were determined on a total of 20 samples (Figs. 5–8): seven from Almansor, comprising three of diatexites, two weakly foliated granitoids and two trondhjemitic veins; four samples from Valverde, corresponding to two pairs of foliated granitoid and non-foliated granitoid; nine samples from Alto de São Bento, comprising two each of two-mica leucogranite, tonalite, porphyritic granite and mafic granular enclaves, and one of granodiorite. Given the complexity and peculiarity of Almansor and Valverde outcrops a drill was used to collect samples. Since many of the rocks occurred as layers, veins and pods, several holes were performed in order to obtain a reasonable amount of sample (average ~500 g/sample). At Alto de São Bento, the minimum weight per sample was 2 kg. Whole-rock geochemical data are reported in Table 1 and analytical techniques are described in Appendix A (I).

4.1. Almansor area

Major and trace element data obtained from the Almansor samples confirm the previous subdivision of three main groups (diatexites, weakly foliated granitoids and trondhjemitic veins) based on field and microscopic observations.

The diatexites correspond to intermediate and acidic rocks ($58<SiO_2<71$ wt.%) with the highest and lowest values of silica corresponding, respectively, to the lowest and highest values of MgO, Al_2O_3, $Fe_2O_3^*$, TiO_2, Na_2O and K_2O (Table 1), while the CaO values are always very low (0.9–1.09 wt.%). All diatexites are peraluminous, with a A/CNK ratio ranging from 1.27 to 1.52 (Fig. 5C), which agrees with an origin from a metasedimentary source. Despite the great variability of SiO_2 values measured in diatexites, their trace element patterns are quite similar (Fig. 6A), all showing a relative enrichment of the most incompatible elements (Th_N/Y_N~20) and moderate negative anomalies of Nb, Eu and Ti (Th_N/Nb_N~10; La_N/Nb_N~5; Eu/Eu*~0.65; Ti_N/Gd_N~0.25).

Considering the major element geochemistry, the weakly foliated granitoids differ from the diatexites by higher values of CaO (3.05; 3.41 wt.%) and Na_2O (4.10; 4.19 wt.%), lower concentrations of K_2O (1.66; 2.28 wt.%) and lower A/CNK ratio ~1.1, revealing a slightly peraluminous nature (Fig. 5C). The trace-element patterns (Fig. 6B)

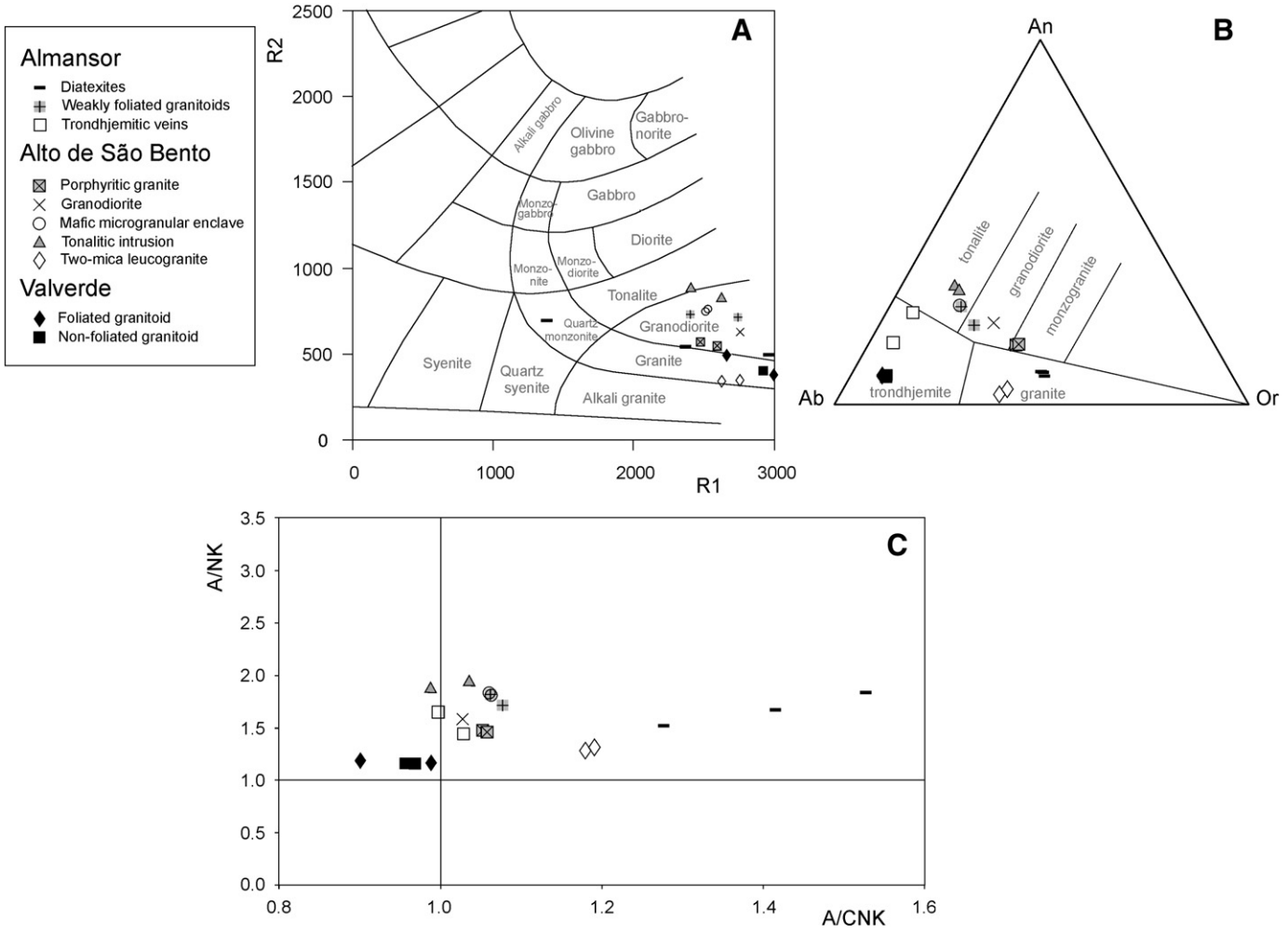

Fig. 5. Diagrams based on major elements for the studied rocks from the three studied areas. (A) Classification for plutonic rocks using the parameters R1 [4Si-11(Na + K) − 2(Fe + Ti)] and R2 [6Ca + 2Mg + Al], calculated from millication proportions after De la Roche et al. (1980); (B) Classification of granitoid rocks according to their normative An–Ab–Or (O'Connor, 1965); (C) Ratios A/CNK and A/NK as defined by Shand (1947).

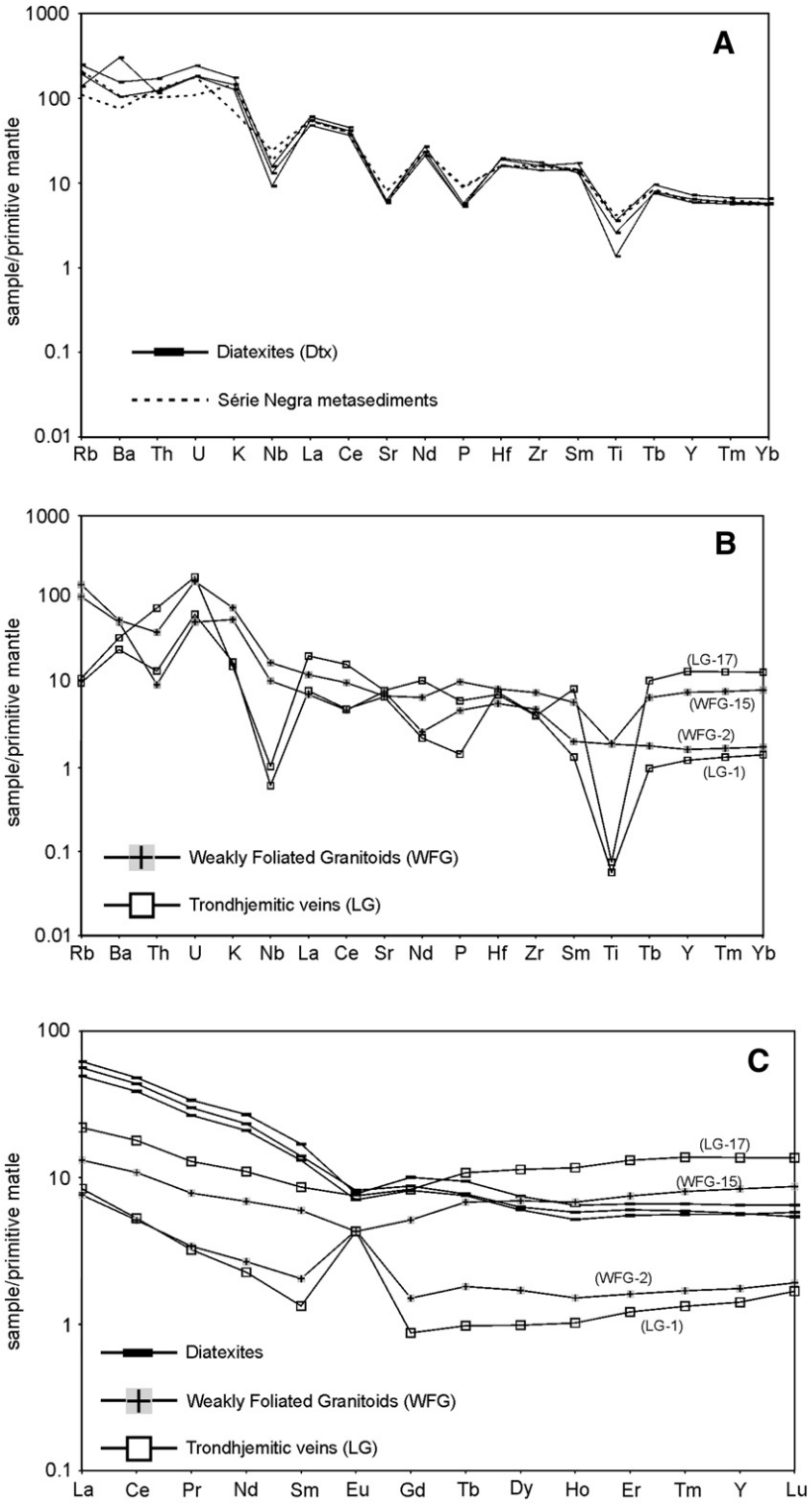

Fig. 6. Samples normalized to primitive mantle (Almansor area). (A) Trace element patterns for diatexites. For comparison trace elements from Ediacaran Série Negra metasedimentary rocks. (B) Trace element patterns for weakly foliated granitoids and trondhjemitic veins. (C) REE patterns for diatexites, weakly foliated granitoids and trondhjemitic veins. Primitive Mantle normalization parameters are from Sun and McDonough (1989).

for the group of weakly foliated granitoids are quite different from those of the diatexites, suggesting an origin other than melting of metasediments. However, there are some features of the trace element data of the weakly foliated granitoids, in particular concerning rare earth elements (REE) and Y, which require a detailed discussion (see Section 7.1). In fact, these rocks show similar concentrations for elements such as V, Sc, Ba, Sr, Rb, Th and La, but, when plotted on a spiderdiagram, discrepancies for REE and Y between samples are observed (Fig. 6B). One of the samples (WFG-2) displays low total REE contents (Fig. 6C), a strong Eu positive anomaly ($Eu/Eu^* = 2.26$) and LREE enrichment ($La_N/Lu_N = 3.98$); the other sample (WFG-15) has $La_N/Lu_N = 1.51$ and shows a V-shaped pattern with a negative slope from La to Eu ($La_N/Eu_N = 3.07$) and a positive slope from Eu to Lu ($Eu_N/Lu_N = 0.49$).

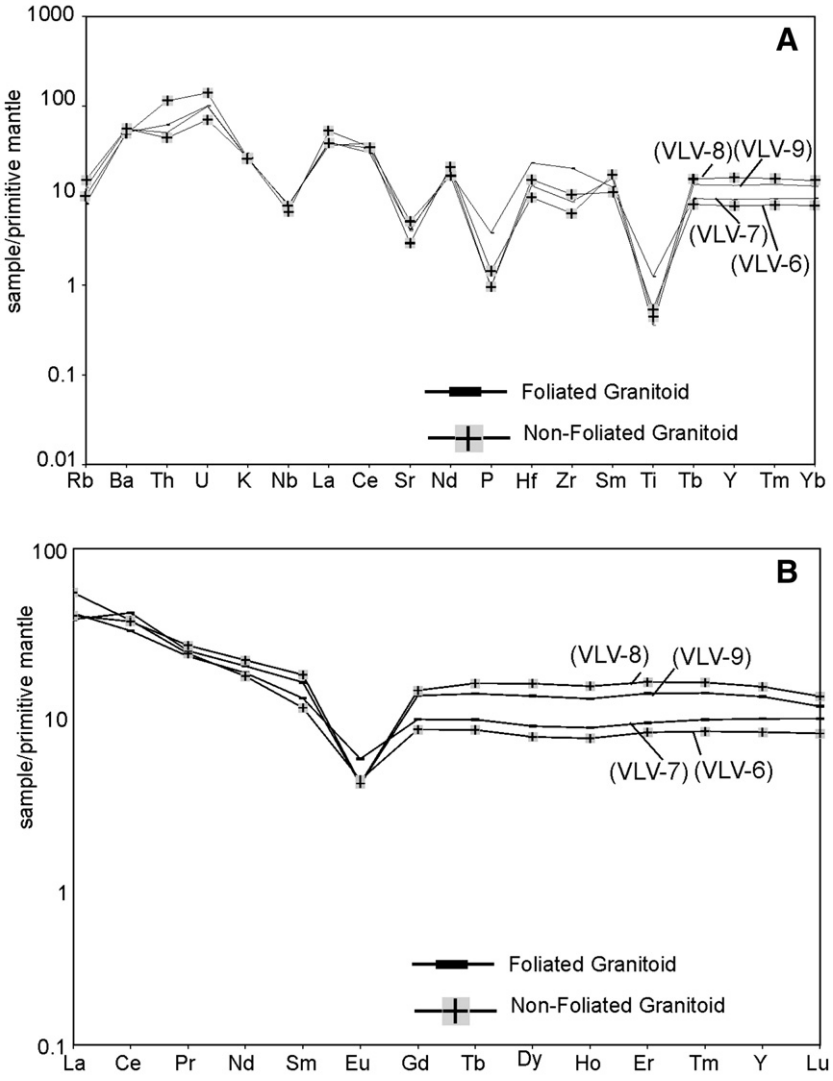

Fig. 7. Samples normalized to primitive mantle (Valverde area). (A) Trace element pattern for foliated and non-foliated granitoids. (B) REE patterns for foliated and non-foliated granitoids. Primitive Mantle normalization parameters are from Sun and McDonough (1989).

The analysed trondhjemitic veins are extremely siliceous rocks (SiO_2 values ~80 wt.%), and display very low contents of MgO, $Fe_2O_3^*$, TiO_2 and K_2O. CaO (1.9–2.9 wt.%) and Na_2O (~4.1 wt.%) concentrations are similar to and higher, respectively, than those obtained in the weakly foliated granitoids. The trondhjemites are transitional between metaluminous and peraluminous compositions, and have

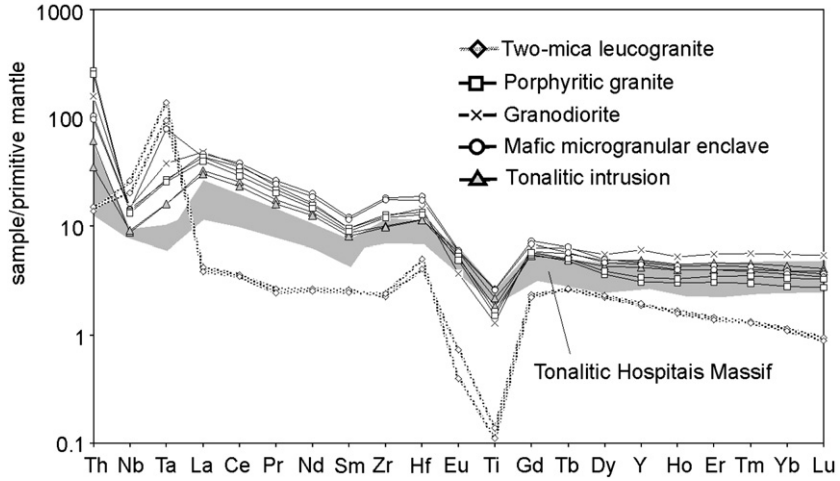

Fig. 8. Primitive mantle normalized trace element pattern for granitoids from Alto de São Bento area. For comparison the data from the Tonalitic Hospitais Massif (Moita et al., 2005b) are also shown. Primitive Mantle normalization parameters are from Sun and McDonough (1989).

Table 1
Whole rock compositions of the studied samples.

	ALMANSOR							VALVERDE				ALTO DE SÃO BENTO								
Sample	Dtx-3	Dtx-4	Dtx-18	WFG-2	WFG-15	LG-1	LG-17	VLV-6	VLV-7	VLV-8	VLV-9	PFPAS	PFMAS	GPAS	ASB-8	ASB-5	ASB-6	ASB-7	ASB-9	ASB-10
Rock type	Dtx	Dtx	Dtx	WFG	WFG	TV	TV	NFG	FG	NFG	FG	PG	PG	2MLG	2MLG	TI	TI	GD	MME	MME
(wt.%)																				
SiO_2	68.18	58.07	70.90	69.61	67.26	77.64	79.01	77.31	74.78	77.88	78.35	70.60	71.98	75.99	74.55	67.28	65.49	70.92	67.37	67.48
TiO_2	0.56	0.76	0.29	0.41	0.42	0.01	0.02	0.12	0.27	0.10	0.08	0.36	0.33	0.03	0.02	0.40	0.47	0.28	0.57	0.56
Al_2O_3	15.02	18.25	14.86	15.45	15.80	13.24	12.41	12.31	12.70	11.78	12.18	14.82	14.49	14.04	14.12	16.13	16.40	14.31	15.94	15.91
$Fe_2O_3^t$	3.37	6.15	2.61	2.97	3.72	0.23	0.22	0.74	2.07	0.82	0.60	2.59	2.46	0.77	0.74	3.61	4.15	2.51	4.09	4.01
MnO	0.06	0.10	0.05	0.04	0.06	0.00	0.00	0.01	0.02	0.01	0.01	0.06	0.05	0.05	0.05	0.07	0.08	0.05	0.08	0.08
MgO	2.54	3.79	1.96	1.26	1.56	0.06	0.09	0.25	0.51	0.39	0.16	0.83	0.77	0.08	0.08	1.30	1.58	0.97	1.36	1.33
CaO	1.08	1.09	0.90	3.37	3.00	2.90	1.92	1.35	1.96	1.20	1.13	2.21	2.10	0.63	0.55	4.01	4.35	2.70	3.51	3.41
Na_2O	3.26	3.42	2.56	4.06	4.12	4.55	4.93	5.82	5.91	5.54	5.74	3.58	3.54	3.90	4.13	4.09	4.33	3.63	4.12	4.15
K_2O	4.12	4.91	3.60	1.66	2.28	0.52	0.46	0.75	0.75	0.76	0.74	3.87	3.78	3.90	3.85	1.46	1.45	2.81	1.73	1.79
P_2O_5	0.11	0.12	0.11	0.10	0.22	0.03	0.13	0.02	0.08	0.03	0.02	0.15	0.13	0.18	0.20	0.11	0.12	0.07	0.19	0.18
LOI	0.87	1.95	1.32	0.57	0.53	0.15	0.34	0.15	0.08	0.25	0.24	0.59	0.50	0.61	0.63	0.52	0.44	0.48	0.61	0.59
TOTAL	99.17	98.62	99.16	99.49	98.96	99.35	99.51	98.82	99.12	98.75	99.23	99.65	100.14	100.19	98.91	99.00	98.87	98.72	99.57	99.50
(ppm)																				
Sc	14	17	7	8	11	<d.l.	1	4	7	11	8	6	6	2	2	8	9	7	8	8
Be	3	5	6	2	1	1	1	2	2	2	2	4	4	16	14	2	2	2	4	5
V	92	145	71	39	48	<d.l.	<d.l.	<d.l.	15	<d.l.	<d.l.	25	23	<d.l.	<d.l.	32	41	26	46	44
Cr	76	115	64	<d.l.	<d.l.	<d.l.	<d.l.	<d.l.	<d.l.	<d.l.	<d.l.	<d.l.	<d.l.	<d.l.	<d.l.	<d.l.	<d.l.	26	24	25
Co	6	20	5	5	7	<d.l.	4	<d.l.	2	1	<d.l.	4	3	<d.l.	<d.l.	6	7	4	8	7
Ni	31	112	111	<d.l.	<d.l.	<d.l.	<d.l.	<d.l.	<d.l.	<d.l.	<d.l.	<d.l.	<d.l.	<d.l.	<d.l.	<d.l.	<d.l.	<d.l.	<d.l.	<d.l.
Cu	15	125	11	12	16	20	<d.l.	<d.l.	<d.l.	<d.l.	<d.l.	<d.l.	47	<d.l.	<d.l.	<d.l.	<d.l.	<d.l.	<d.l.	<d.l.
Zn	<d.l.	<d.l.	<d.l.	<d.l.	<d.l.	<d.l.	<d.l.	<d.l.	<d.l.	<d.l.	<d.l.	<d.l.	<d.l.	<d.l.	49	45	33	<d.l.	34	39
Ga	20	28	17	19	22	12	11	17	18	14	17	15	15	14	20	20	20	18	24	23
Ge	1.7	1.6	1.2	1.5	1.7	1.1	1.3	1.3	1.6	1.2	1.5	1	<d.l.	2	3.1	1.3	1.5	1.4	1.2	1.3
As	11	<d.l.	9	<d.l.	<d.l.	<d.l.	32	<d.l.	<d.l.	<d.l.	<d.l.	<d.l.	<d.l.	<d.l.	<d.l.	<d.l.	<d.l.	<d.l.	<d.l.	<d.l.
Rb	123	156	87	69	97	6	7	6	5	10	8	177	156	287	321	67	58	168	211	211
Sr	122	131	132	169	151	147	175	109	89	62	86	197	182	18	10	293	296	123	196	191
Y	26.6	32.8	29.2	7.5	35.9	5.6	63.9	35.0	41.2	72.3	59.2	14	15	9	8.8	22.3	19.0	27.6	21.2	20.4
Zr	194	178	159	56	88	48	46	115	227	71	96	143	134	25	27	112	109	137	204	195
Nb	9.3	11.1	6.5	7.7	12.7	0.4	0.7	4.7	5.6	5.5	5.7	10	9	14	18.6	6.2	6.5	10.6	10.3	10.1
Sn	3	2	3	2	2	<d.l.	<d.l.	3	4	7	5	7	5	22	19	2	4	9	6	5
Cs	4.0	4.2	2.5	2.4	3.2	0.2	0.4	0.2	−0.1	0.3	0.3	12.4	9.1	28.1	23.7	4.7	6.4	20.2	24.2	21.2
Ba	727	1,080	2,100	377	398	178	247	333	352	343	375	692	489	18	7	444	472	563	155	159
La	33.97	42.74	39	5.25	9	5.80	15	37	28	27	26	29.6	27.2	2.9	3	22	21	33	32	30
Ce	69.2	85.8	78	9.2	19	9.4	32	66	57	64	73	56.0	51.3	6.4	6	45	41	65	68	62
Pr	7.39	9.37	8	0.94	2	0.89	4	6	6	7	7	6.00	5.58	0.73	1	5	4	6	7	7
Nd	28.5	36.7	32	3.6	9	3.1	15	23	24	29	26	21.1	19.8	3.6	3	18	17	22	27	25
Sm	5.85	7.56	6	0.91	3	0.59	4	5	6	8	7	4.2	4.0	1.2	1	4	4	4	5	5
Eu	1.19	1.31	1	0.74	1	0.73	1	1	1	1	1	0.89	0.82	0.12	0	1	1	1	1	1
Gd	4.90	6.01	5	0.90	3	0.52	5	5	6	8	8	3.3	3.4	1.4	1	3	3	4	4	4
Tb	0.82	1.02	0.8	0.20	0.7	0.11	1.2	0.9	1.0	1.7	1.4	0.5	0.5	0.3	0.3	0.6	0.5	0.7	0.7	0.6
Dy	4.45	5.52	5	1.26	5	0.73	8	5	6	11	9	2.7	2.8	1.6	2	4	3	4	4	3
Ho	0.85	1.07	1	0.25	1	0.17	2	1	1	2	2	0.5	0.5	0.3	0	1	1	1	1	1
Er	2.66	3.19	3	0.77	4	0.58	6	4	4	7	6	1.5	1.7	0.7	1	2	2	3	2	2
Tm	0.42	0.49	0.44	0.13	0.60	0.10	1.02	0.58	0.69	1.15	0.99	0.22	0.26	0.10	0.10	0.33	0.30	0.42	0.32	0.28
Yb	2.78	3.22	3	0.87	4	0.70	7	4	5	7	6	1.4	1.6	0.6	1	2	2	3	2	2
Lu	0.43	0.48	0.40	0.14	0.65	0.12	1.01	0.57	0.69	0.95	0.82	0.20	0.24	0.07	0.07	0.30	0.29	0.40	0.27	0.25
Hf	6.0	5.9	5	1.8	3	2.4	2	5	7	3	4	4.1	4.0	1.3	2	4	4	4	6	5
Ta	0.67	1.15	0.6	0.80	1.3	0.09	0.1	0.8	0.5	0.8	0.8	1.1	1.0	3.9	5.6	0.6	0.7	1.6	1.1	3.2
W	0.9	1.1	0.7	0.5	0.6	0.8	1.0	<d.l.	<d.l.	0.7	0.5	<d.l.	2	1	2.6	0.7	0.6	1.1	2.6	0.8
Tl	0.79	0.88	1	0.40	0	<d.l.	0	0	0	0	0	1.8	1.4	2.1	2	0	0	1	1	1
Pb	22	29	16.9	26	16.1	13	15.3	<d.l.	<d.l.	<d.l.	<d.l.	20	18	23	24.6	48.6	12.3	18.7	19.6	21.8
Bi	0.2	0.2	0.7	0.5	0.3	0.1	0.7	0.3	0.6	0.3	0.4	5.2	2.7	28.2	7.5	0.6	0.4	0.3	0.4	0.2
Th	10.28	14.29	9.8	0.82	3.4	1.19	6.7	9.5	5.2	3.7	4.2	23.0	21.3	1.3	1	5	3	13	9	8
U	3.85	5.09	3.8	1.14	3.5	1.40	3.9	2.9	2.1	1.5	2.1	2.7	2.9	9.7	4	1	1	5	3	4

Almansor: Dtx- Diatexite (Dtx-3 and Dtx-18 are monzonites; Dtx-4 is quartz-monzonite); WFG- weakly foliate granitoid (WFG-2 is tonalite and WFG-15 granodiorite); TV — Trondhjemitic veins; Valverde: FG — foliated granitoid (trondhjemite), NFG-non foliated granitoid (trondhjemite); Alto de São Bento: PG — porphyritic granite; 2MLG — two-mica leucogranite; TI — tonalitic intrusion, GD — granodiorite, MME — mafic microgranular enclave (tonalite). LOI — Loss on ignition; d.l. — detection limit.

A/CNK ratios (0.99 and 1.03) very close to 1. The very high silica values (greater than in the composition of the granite minimum melt) may indicate that some quartz accumulation took place.

The trondhjemite samples have similar contents of several trace elements and their spiderdiagrams share some relevant features, such as strong negative Nb and Ti anomalies (Th_N/Nb_N: 22.86; 75.95 and Sm_N/Ti_N: 23.85; 115.55). However, differences regarding REE and Y (Fig. 6B) were also present in these samples.

If the REE patterns of trondhjemites and weakly foliated granitoids (Fig. 6C) are considered together, two pairs of samples may be defined according to the similarities between those patterns: each pair includes one sample of trondhjemitic vein and one sample of weakly foliated granitoid (LG-1/WFG-2 and LG-17/WFG-15). Probably, this grouping results from the strong influence on REE geochemistry of both lithologies exerted by the same mineral phases, as it will be discussed below.

4.2. Valverde area

With the purpose of identifying distinct features between lithologies, four samples were collected in this outcrop grouped as spatially related

pairs: one sample of each pair is of non-foliated granitoid and the other is a foliated granitoid less than one metre away.

However, the studied samples from Valverde area have very similar values for most major element oxides, including high SiO_2 (>75%) and Na_2O (>5.5%) concentrations, accompanied by low CaO (<2.0%) and K_2O (<0.8%) values, consistently with their classification as trondhjemites. No systematic geochemical differences were detected: all samples are metaluminous, with A/CNK ratios between 0.9 and 1 (Fig. 5C); the trace element contents and normalized REE patterns are also quite similar (Fig. 7A and B), with negative Nb and Ti anomalies (Th_N/Nb_N: 5.61–16.96; Ti_N/Gd_N: 0.03–0.13). One of the few discrepancies is the higher Zr contents in FLD-7 (227 ppm) in comparison with the other samples (<115 ppm). The REE patterns display slight LREE enrichment (La_N/Lu_N: 3.08–8.87) and pronounced Eu negative anomalies (Eu/Eu* between 0.24 and 0.49). Both samples (VLV-8 and VLV-9) of one pair exhibit higher contents of HREE than the other pair and consequently have the lowest La_N/Lu_N ratios. Therefore, geochemical differences seem to be more between spatially separated pairs, than between foliated and non-foliated granitoids.

4.3. Alto de São Bento area

Granitoids from Alto de São Bento area, with the exception of two-mica leucogranites, are metaluminous to slightly peraluminous (A/CNK: 0.99–1.06, Fig. 5C). They all have SiO_2 over 65.5%, and display negative correlations between silica and MgO, CaO, Fe_2O_3* or TiO_2. Spiderdiagrams (Fig. 8) and normalized REE plots of these lithologies, showing general enrichment of the most incompatible elements (e.g. La_N/Lu_N: 7.86 to 25.53) and pronounced negative Nb and Ti anomalies (Th_N/Nb_N: 3.83–19.84; Ti_N/Gd_N: 0.2–0.46), are all coherent and consistent with a calc-alkaline signature. This agrees with the common occurrence of calc-alkaline magma suites with Variscan ages in the Ossa–Morena Zone, specially in its southern and western sectors, as has been reported in previous works (Santos et al., 1990; Castro and De La Rosa, 2002; Casquet and Galindo, 2004; Antunes, 2006; Moita, 2007).

Two-mica leucogranites exhibit markedly different geochemical features compared to the other granitoid rocks of Alto de São Bento, pointing to a different origin: they are clearly peraluminous (A/CNK ~ 1.2, Fig. 5C), have significantly lower contents of most of the usually incompatible elements (except Rb, Nb and Ta), show stronger negative Ti and Eu anomalies and display flatter REE patterns (La_N/Lu_N: 4.34 and 4.43).

5. Timing relationships

Despite that no radiometric dating has been performed on samples from the studied lithologies from Almansor and Valverde, it is possible to put some time constraints to the events that they represent by taking into account the regional geological framework and their field relationships with the surrounding geological units.

Tonalitic enclaves, found inside the weakly foliated granitoids from Almansor, were probably derived from a voluminous syn-tectonic intrusion in the neighbourhood — the Tonalitic Hospitais Massif (Carvalhosa and Zbyszewski, 1994; Moita et al., 2005a,b). An Ar–Ar age of 323 ± 5.2 Ma obtained on igneous amphibole from the Hospitais tonalite, was interpreted as representing a cooling age after crystallization (Moita et al., 2005c). Considering not only the presence of the enclaves, but also the structural record showing that Almansor lithologies are syn-tectonic, the weakly foliated granitoids should be younger than the Hospitais massif.

For the Valverde area, besides the field relationships already described, Chichorro (2006) obtained a monazite SHRIMP U–Pb date of 322 ± 6.8 Ma, from the felsic orthogneisses, which was claimed to be the age of high temperature metamorphism (and related migmatization) recorded by these rocks.

Using a sample of two-mica leucogranite from Alto de São Bento, an internal Rb–Sr errorchron (whole rock, plagioclase, muscovite and biotite) of 322 ± 16 Ma was obtained (Moita, 2007). Despite the high MSWD (13) and error that do not allow a clear conclusion from this result, it must be noticed that the errorchron in the leucogranite points to an age very similar to those obtained for the magmatic crystallization at Hospitais (and Almansor?) and partial melting at Valverde.

In summary, high-temperature metamorphism, as well the genesis and crystallization of very different types of granitoid magmas in the Almansor, Valverde and Alto de São Bento areas (located between Montemor-o-Novo and Évora), seem to have occurred in a period between 320 and 330 Ma, which marks a significant thermal event in this sector of the Ossa–Morena Zone.

6. Sr and Nd isotopic data

Sr and Nd isotopic analyses were performed on six samples from Almansor area (two samples each from diatexites, weakly foliated granitoids and trondhjemitic veins), four samples from the Valverde area (two pairs of foliated and non-foliated granitoids) and four samples from the Alto de São Bento area (two-mica leucogranite,

Table 2
Rb–Sr and Sm–Nd isotopic data from the studied lithotypes.

Sample	r.t.	$^{87}Rb/^{86}Sr$	(2σ)	$^{87}Sr/^{86}Sr$	(2σ)	$^{87}Sr/^{86}Sr_i$	$^{147}Sm/^{144}Nd$	(2σ)	$^{143}Nd/^{144}Nd$	(2σ)	$^{143}Nd/^{144}Nd_i$	εNd_i
Almansor												
Dtx-4	Dtx	3.452	0.098	0.728440	(39)	0.712569	0.125	0.004	0.512029	(14)	0.511765	−8.9
Dtx-18	Dtx	1.909	0.054	0.720399	(37)	0.711621	0.113	0.003	0.511984	(12)	0.511745	−9.3
WFG-2	WFG	1.182	0.033	0.712754	(36)	0.707321	0.153	0.004	0.512344	(14)	0.512021	−3.9
WFG-15	WFG	1.860	0.053	0.715735	(29)	0.707184	0.202	0.006	0.512366	(11)	0.511940	−5.5
LG-1	TV	0.118	0.003	0.708328	(35)	0.707785	0.115	0.003	0.512272	(11)	0.512028	−3.8
LG-17	TV	0.116	0.003	0.712318	(37)	0.711786	0.161	0.005	0.512251	(20)	0.511910	−6.1
Valverde												
VLV-6	NFG	0.159	0.005	0.710031	(33)	0.709298	0.132	0.004	0.512340	(12)	0.512061	−3.1
VLV-7	FG	0.163	0.005	0.709884	(35)	0.709137	0.151	0.004	0.512358	(18)	0.512038	−3.6
VLV-8	NFG	0.467	0.013	0.711198	(44)	0.709052	0.167	0.005	0.512376	(17)	0.512023	−3.9
VLV-9	FG	0.269	0.008	0.710294	(38)	0.709057	0.163	0.008	0.512375	(12)	0.512030	−3.7
Alto de São Bento												
ASB-6	TI	0.567	0.016	0.709070	(38)	0.706463	0.142	0.004	0.512277	(10)	0.511976	−4.8
ASB-7	GD	3.96	0.110	0.724928	(36)	0.706731	0.110	0.003	0.512177	(10)	0.511944	−5.4
ASB-8	2MLG	92.71	2.620	1.145137	(7)	0.718939	0.202	0.006	0.512280	(24)	0.511853	−7.2
ASB-9	MME	3.118	0.088	0.719808	(33)	0.705472	0.112	0.003	0.512402	(15)	0.512165	−1.1

See Appendix for analytical procedures. Uncertainties for the $^{87}Sr/^{86}Sr$ and $^{143}Nd/^{144}Nd$ are 2σ (mean) errors in the last two digits. εNd_i values at the time of intrusion are calculated relative to CHUR with present day values of $^{143}Nd/^{144}Nd = 0.512638$ and $^{147}Sm/^{144}Nd = 0.1967$ (Jacobsen and Wasserburg, 1980). (i): initial. Rock type (r.t.) abbreviations as in Table 1.
Rock type abbreviations as in Table 1.

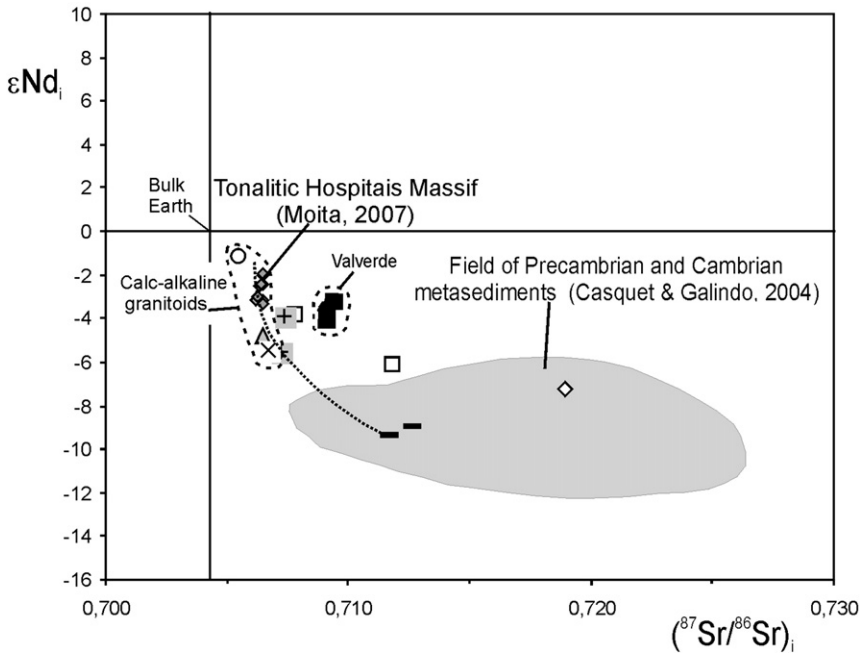

Fig. 9. Plot of $\varepsilon Nd_{(323\ Ma)}$ versus $^{87}Sr/^{86}Sr_{(323\ Ma)}$ for Almansor, Valverde and Alto de São Bento granitoids. The data for Precambrian and Cambrian metasediments from OMZ are from Casquet and Galindo (2004) and for tonalitic Hospitais massif are from Moita (2007). The dotted curve represents the hypothetical curve for simple mixing between the tonalitic mafic end member (from Hospitais massif) and a diatexite crustal end member. Symbols as in Fig. 5.

granodiorite, tonalite and mafic microgranular enclave). The data are reported on Table 2 and analytical techniques are described in Appendix A (II). The $(^{87}Sr/^{86}Sr)_i$ ratio and εNd_i for the samples were recalculated for 323 Ma, considering the geochronological constraints discussed above.

In Fig. 9, diatexites and weakly foliated granitoids from Almansor plot separately, as expected from their major and trace element compositions: diatexites have high $^{87}Sr/^{86}Sr_i$ (0.711621; 0.712569) and negative εNd_i (−9.3; −8.9), in agreement with a metasedimentary source; weakly foliated granitoids display lower $^{87}Sr/^{86}Sr_i$ (0.707184; 0.707321) and less negative εNd_i (−3.9; −5.5), supporting that their origin is distinct from that of the diatexites. The isotopic signatures of trondhjemitic veins show significant differences amongst samples, since LG-1 lies very close to the weakly foliated granitoids ($^{87}Sr/^{86}Sr_i = 0.707785$; $\varepsilon Nd_i = -3.8$), but LG-17 has $^{87}Sr/^{86}Sr_i$ (0.711786) identical to the Sr isotope ratios in diatexites and a εNd_i (−6.1) value overlapping those found in weakly foliated granitoids.

Foliated and non-foliated granitoids from Valverde show quite similar isotope data ($^{87}Sr/^{86}Sr_i$ ranges from 0.709052 to 0.709298 and εNd_i from −3.1 to −3.9, considering all samples), confirming that they cannot be discriminated by geochemical criteria.

Lithologies from the Alto de São Bento area have very distinct isotopic features suggesting the involvement of different sources. The two-mica leucogranite sample exhibits the signature of high radiogenic strontium ($^{87}Sr/^{86}Sr_i = 0.718939$) and a negative εNd_i value (−7.2); the mafic microgranular enclave ($^{87}Sr/^{86}Sr_i = 0.705472$; $\varepsilon Nd_i = -1.1$) plots near the Bulk Earth composition; granodiorite and tonalite exhibit intermediate values (granodiorite, $^{87}Sr/^{86}Sr_i = 0.706731$; $\varepsilon Nd_i = -5.4$; tonalite, $^{87}Sr/^{86}Sr_i = 0.706463$; $\varepsilon Nd_i = -4.8$).

7. Discussion

7.1. Almansor area

7.1.1. Genesis of diatexites

Diatexites present several features indicative of anatexis of a metasedimentary source, namely the presence of restitic bodies with biotite-rich (and, sometimes, cordierite-bearing) modal compositions, markedly peraluminous compositions and an isotopic signature with high $^{87}Sr/^{86}Sr_i$ and low εNd_i. Additionally, trace-element patterns of Almansor diatexites and upper crustal materials (Rudnick and Gao, 2003) show very strong similarities; those evident on the spiderdiagrams are also observed in the Série Negra paragneisses (Ediacarian sediments; Pereira et al., 2006b; Fig. 6A) from the Évora Massif. In particular, Rb, Ba and Sr contents from diatexites closely match a pelitic source, according to the parameters (Rb>100 ppm; Ba<600–1000 ppm; Sr<300–400 ppm) proposed by Miller (1985). The Sr and Nd isotopic data from the diatexites lie in the same range of the values obtained from Ediacaran Série Negra and Cambrian metasediments from several regions of the Ossa–Morena Zone (Casquet and Galindo, 2004). Consequently, Série Negra metasediments are interpreted as the source of diatexite magma. They constitute a thick sequence of metapelites in OMZ (Carbonell et al., 2004) largely composed of lithologies that are susceptible to dehydration, and subsequent partial melting, with temperature increase under realistic crustal conditions (e.g. Patiño Douce, 1999).

The significant differences in major element compositions amongst the diatexite samples are probably a result of variation in the proportion of refractory material between diatexites. The refractory material was most likely biotite, but in some cases cordierite, dispersed throughout the melt. During magmatic crystallization, and subsequent cooling, the restitic minerals, given its "igneous" appearance, seem to have texturally re-equilibrated with the newly formed minerals, erasing most of the petrographic evidence of derivation from a metamorphic protolith. Therefore the quartz-monzonitic diatexite (Dtx-4) seems to have had a greater preservation of biotite (+/− cordierite) during anatexis and melt flow processes, compared to the monzogranitic diatexite (Dtx-3).

7.1.2. Melting conditions

The strong resemblance between the trace element patterns of diatexites and the most likely source materials can be explained by incomplete separation between the melt and the residuum or by high degrees of partial melting. The heat necessary to trigger melting was most probably provided by the intrusion of mantle derived gabbro-dioritic and tonalitic plutons widespread throughout the EHMT.

In order to constrain the temperature of melting, the empirical Zr thermometer equation of Watson and Harrison (1983), which provides a simple but robust method (Miller et al., 2003), was used. That equation is expressed as $T_{Zr} = 12900/2.95 + 0.85\ M + \ln(496000/Zr_{magma})$, where $M = (Na + K + 2Ca)/(Al * Si)$ using cationic fractions, Zr_{magma} is the concentration of the element in ppm and T_{Zr} represents the temperature in °K. The obtained values indicate temperatures ranging from 836 to 862 °C for the formation of diatexites. Although relatively high, these temperatures estimates are expected for anatectic magmas, considering realistic pressure values and the onset of biotite dehydration (Miller et al., 2003).

However, one can argue that, at the temperatures obtained with the Zr thermometer equation, biotite should be a reacting phase and, therefore, garnet and cordierite should be widespread in the restitic parts of the diatexites, instead of being represented only by scarce relics of cordierite. One possibility is the influence of volatile components, other than water, in the stability of biotite; in particular, increasing $F/(F+OH)$ is expected to raise the temperature of biotite dehydration melting (Hensen and Osanai, 1994). A second hypothesis is that the garnet and the cordierite that would have formed under the peak temperatures reacted later with the melt (and/or the fluids liberated at the final stages of magmatic crystallization), leading to their replacement by biotite in the diatexites. The information obtained so far does not allow to determine which is the likely explanation for the absence of garnet and scarcity of cordierite.

The pressure conditions of the melting event was probably within or close to the interval 4-9 kbar estimated for the crystallization of the Hospitais Massif (Moita, 2007). As discussed in previous sections, this intrusion is spatially related and quasi-contemporaneous with generation of diatexites. Similar P-T conditions have been determined by several authors (Patiño Douce et al., 1997; El-Biad, 2000; Díaz Azpiroz et al., 2004) for the Aracena metamorphic belt, where migmatites with ages around 330 Ma (328 ± 4 Ma; 331 ± 27 Ma; Castro et al., 1999a) are described.

7.1.3. Genesis of weakly foliated granitoids

The analysed samples of the tonalitic–granodioritic weakly foliated granitoids are almost indistinguishable from each other by their petrographic and major element characteristics; however, there are some relevant differences in trace element patterns that will be discussed below. As a group, the weakly foliated granitoids are clearly distinct from the diatexites, suggesting that they may not represent simple products of melting of metapelitic rocks. Particularly, the metaluminous character, the relatively high CaO contents, the low Rb/Sr ratios and even the trace-element patterns precludes a source like the Série Negra metasediments.

Furthermore, the Sr and Nd isotopic data plot away from the diatexites and outside the vast field of Ediacaran and Cambrian metasedimentary rocks from the OMZ (Casquet and Galindo, 2004). Instead, the weakly foliated granitoids display Sr and Nd signatures near the field of the calc-alkaline granitoids that occur within the EHMT (Fig. 9; Moita, 2007). These plutonic rocks were interpreted as the result of fractional crystallization from primitive mafic magmas, produced in the upper mantle affected by supra-subduction enrichment, plus mixing with variable proportions of crustal melts (Moita et al., 2005b; Moita, 2007).

Taking into consideration the isotopic similarity and the probable contemporaneity between the weakly foliated granitoids and the calc-alkaline magmatic suite in the region, it is reasonable to admit a similar origin. Therefore, the weakly foliated granitoids could also be interpreted as the result from superposition of fractional crystallization and magma mixing, with the diatexites likely representing the crustal melts that have been involved in the mixing process. Variation in the proportions of the mixture end-members, as shown in Fig. 9, can explain the slightly different values of εNd_i (whilst Sr isotope ratios are almost equal) between the weakly foliated granitoids since they plot in the upper sector of the proposed mixing curve, where its slope is almost vertical.

As described in Section 4.1, there are some differences amongst samples of weakly foliated granitoids, concerning REE and Y contents. REE patterns similar to that displayed by sample WFG-2 have been interpreted as resulting from strong fractionation (Jung et al., 1999). Furthermore, REE normalized values for WFG-2 also suggest accumulation of plagioclase and zircon: plagioclase explains the La–Sm fractionation and the positive Eu anomaly (Fig. 6B and C), while the role of zircon is indicated by the positive Zr and Hf anomalies and the progressive enrichment of HREE along the segment Ho-Lu. If the addition of apatite occurs an increase of REE and Y concentrations, and a decreasing and eventually erasure of the Eu positive anomaly, is expected (Fujimaki, 1986; Bea, 1996; Zeng et al., 2005). As such, accumulation of apatite would mask the effects of magma fractionation and accumulation of REE-poorer phases. The described features that would result from "addition" of apatite match the REE pattern revealed by sample WFG-15. The hypothesis that the main differences between WFG-2 and WFG-15 geochemistry result from apatite (possibly together with minute amounts of xenotime, which would explain why differences are more important in HREE) are further supported by the higher concentration of P_2O_5 in WFG-15.

7.1.4. Genesis of trondhjemitic veins

Trondhjemitic veins are metaluminous to weakly peraluminous and have low Rb concentrations and low Rb/Sr and Rb/Ba ratios and high Sr/Ba ratios, precluding an origin from anatexis of metapelites. Despite the low CaO concentrations when compared to most of the igneous lithologies, they are above the expected values for melts generated from metapelitic protoliths (Miller, 1985). In accordance, trace-element patterns and isotopic signatures of the Almansor hololeucocratic veins are distinct from those of supra-crustal materials or Série Negra metasediments.

When their REE and Y compositions are considered, differences between samples of trondhjemitic veins are greater than between them and the weakly foliated granitoids, which suggests some affinity between the two lithologies. Even the intra-group discrepancies have the same characteristics and, as such, may be explained in an identical way; participation of "accumulated" minerals, like plagioclase, zircon and apatite, and the masking effect of the phosphate phase when present in larger proportions. The "accumulation" is not, in this case, necessarily the result of segregation during crystallization of a magma, since it is plausible that some interaction, either chemical or mechanical, between trondhjemitic melt and its host environment had occurred. In fact, sample LG-17 – which exhibits a REE pattern probably influenced by apatite and shows, compared to the other trondhjemite sample, higher concentrations of REE and Y (and also of Th and U) – was collected in a thin vein (width: ~3–4 cm) inside diatexite.

Previous works concluded that, in some instances, trondhjemites may result from anatexis of metabasic (e.g. Defant and Drummond, 1990) or metasedimentary source rocks (Patiño Douce and Harris, 1998). However, as emphasized before, an origin from a metapelitic source should be discarded for the Almansor trondhjemitic veins. A process involving melting of a mafic source also seems unlikely in this case, since εNd in mafic metamorphic rocks from close areas, obtained in amphibolites from the Évora Massif (Pereira et al., 2006c), are characterized by positive values, whilst the εNd values in the trondhjemitic veins are negative. In contrast, partial melting of quartz–feldspar rich rocks (e.g. greywackes) under water saturated conditions (Sawyer and Barnes, 1988; Barbey et al., 1989; Johannes et al., 1995; Jung et al., 1999) would be a more plausible mechanism for anatexis, taking into account some relevant geochemical features of the Almansor hololeucocratic veins: namely, the low K contents of the trondhjemites and the trace element pattern displayed by sample LG-1 could be explained in this way.

However, considering the affinities between the trace element contents of weakly foliated granitoids and trondhjemitic veins, the hypothesis of derivation of the more felsic compositions by crystal fractionation from tonalitic–granodioritic magma must be considered. If biotite and ilmenite had a key role in the fractionating assemblage, strong impoverishment in K, Ti, Nb and Ta, accompanying SiO_2 enrichment, as observed in the trondhjemites, would be an expected result.

The match of initial Sr and Nd isotope compositions of the trondhjemite sample LG-1 with those of the weakly foliated granitoid WFG-2 corroborates the suggestion of a derivation by fractional crystallization, with preservation of the isotopic signature of the parental magma by the product of differentiation (e.g. Clarke, 1992). This interpretation is strengthened by the spatial relationship of those two samples; LG-1 represents a vein (or segregation?) within the weakly foliated granitoid where WFG-2 was collected.

Sample LG-17, in contrast, shows a dual isotopic behaviour: εNd_i is similar to values found in weakly foliated granitoids, but $^{87}Sr/^{86}Sr_i$ ratio is much higher and overlaps the Sr isotope compositions of the diatexites. This discrepancy may be the result of a post-magmatic re-equilibrium affecting the isotope ratio of Sr much more effectively than that of Nd, in a similar way to what was proposed by Holden et al. (1987) and Lesher (1990). Taking into account that sample LG-17 is a thin vein within diatexite, this explanation becomes plausible in this case also. Therefore, the dual isotopic signature results from an enrichment in radiogenic Sr, due to the composition of the rock (diatexite) that hosts the vein, whilst the Nd isotope signature preserves the memory of its magmatic origin.

7.1.5. Compositional layering: evidence for in situ melting or for mixing/mingling processes?

From the previous discussion in this section the three main lithologies cropping out at Almansor are best explained by very different processes accounting for their genesis, instead of a single mechanism relating them all simply by crustal anatexis. In this way, the layered structure observed in this area, rather than testifying *in situ* migmatization, seems to correspond to complex mingling and mixing of magmas injected into an active shear zone, as proposed by Pawley et al. (2002) to explain the compositional layering in Woodstock monzogranite (Pilbara Craton, NW Australia). The role of accessory phases and the occurrence of local post-magmatic isotopic re-equilibrium add further geochemical complexity.

7.2. Valverde area

7.2.1. What do foliated and non-foliated granitoids represent? In situ melting vs. melt segregation hypotheses

The field relationships at the Valverde outcrop can easily be interpreted to indicate that foliated granitoids represent a metamorphic protolith and the pods and veins with non-foliated structure/texture correspond to anatectic melts. However, petrographic and geochemical (elemental and isotopic) information show that the two rocks (both displaying trondhjemitic compositions) have essentially identical features, except, of course, for their mesoscopic appearance. Two hypotheses can be put forward: 1) this outcrop is a migmatitic domain where partial melting occurred, but this process did not cause any geochemical fractionation between source rock and anatectic melt; 2) the foliation would be mainly a magma flow structure (although probably influenced by the tectonic stress field), rather than a (pre-melting) metamorphic anisotropy, and the two types of trondhjemite would correspond to local segregations from an initial precursor magma.

The first hypothesis is favoured by field observations, but requires conditions where no partitioning occurred for a very wide range of elements (both for major and trace elements with usually very different degrees of incompatibility). The second hypothesis fits well the absence of microscopic evidence for earlier sub-solidus deformation in the foliated granitoids and to the identical geochemical features shown by the two rocks. Although considered rare (Miller et al., 1988), segregation structures can be preserved in granitic rocks (Sawyer, 2000) and, taking into account the geochemical and petrographic information, the Valverde outcrop could be syn-crystallization melt segregation structures.

If the second hypothesis is accepted, the metaluminous nature of the rocks seems to preclude that the magma from which they crystallized was related to partial melting of a metasedimentary source. The Valverde trondhjemites should, therefore, represent either a very evolved stage of differentiation from a mafic magma, or anatexis of an orthogneiss. The existence of Cambrian felsic orthogneisses (Chichorro, 2006) in the neighbouring area could be regarded as a possible protolith, as will be investigated in ongoing geochemical studies.

7.3. Alto de São Bento

7.3.1. Interaction of anatectic melts with mantle derived magmas?

Most of the lithologies identified at the Alto de São Bento area exhibit metaluminous to slightly peraluminous compositions. They display calc-alkaline signatures and may all be related by fractional crystallization processes. Also, their trace element signatures have strong similarities with the coeval Tonalitic Hospitais Massif (Fig. 8; Moita et al., 2005b) which could, therefore, represent the more primitive end of the same liquid line of descent. According to elemental geochemistry, the fractionation of plagioclase plus hornblende can be regarded as the main mechanism leading to the evolution from a tonalitic (Hospitais) magma to the more silicic compositions found at Alto de São Bento.

Nevertheless, the isotopic data cannot be explained by fractional crystallisation alone, requiring a more complex model.

As discussed in previous sections, field relationships observed at the Almansor outcrop represent conspicuous mechanical interaction of distinct melts; additionally the geochemical features of the Almansor lithotypes suggest that the melts probably also interacted chemically. Therefore, the geological evidence obtained at Almansor points to a significant participation of mingling and mixing in magmatic diversification within the EHMT.

At Alto de São Bento, field evidence of mingling, although not as important as at Almansor, is also suggested by the presence of mafic microgranular enclaves within porphyritic granite. The lithologies that occur in the former area correspond, in general, to distinct bodies without the abundance of interpenetrations that can be seen at Almansor, revealing greater degrees of homogenization of the magma pulses that were emplaced at Alto de São Bento. Therefore, and considering that fractional crystallisation could not have worked alone, it is likely that magma mixing, involving variable proportions of mafic and felsic poles, took place at deeper crustal levels.

The composition of diatexites, cropping out at Almansor, fits well as the crustal endmember of the simple mixing curve defined by the calc-alkaline intrusives. Neodymium and Sr isotope ratios obtained from the analysis of a sample of mafic microgranular enclave (of modal tonalitic composition), hosted by the Alto de São Bento porphyritic granite, was used as "mantle" endmember, since it has $^{87}Sr/^{86}Sr_i$ and εNd_i very close to the values found in the gabbros from the EHMT (in fact, the εNd_i of the enclave is even slightly higher), suggesting that it represents the magmas least affected by chemical interaction with crustal material in the studied areas. According to the mixing calculations, the granodiorite and the tonalitic facies described in Section 3.3 should result from a hybridization process in which the felsic crustal component corresponds to 40% and 30% of the mixture, respectively.

The strongly peraluminous granite (two-mica leucogranite) that occurs at Alto de São Bento has a high radiogenic Sr isotopic signature,

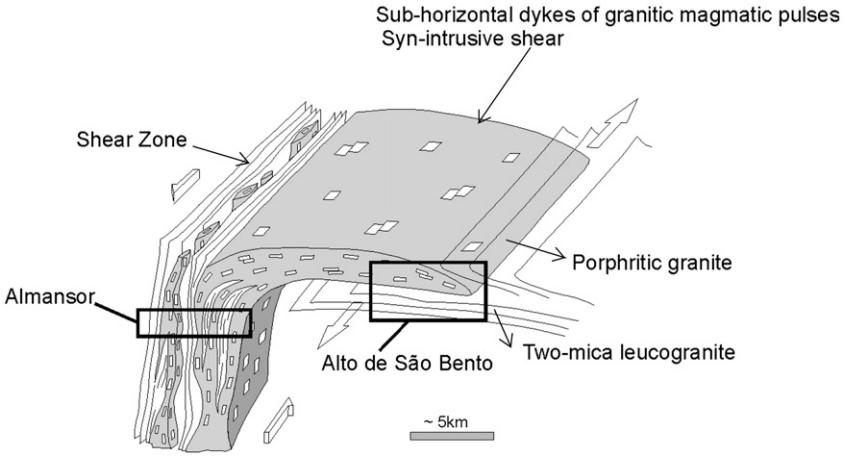

Fig. 10. Interpretation diagram to explain the relation between two areas (Almansor and Alto de São Bento) characterized by different mesoscopic features, but similar geochemical evolutionary processes (adapted from Stålfors and Ehlers, 2005).

indicating that it crystallized from a melt generated by anatexis of lithologies of supracrustal provenance (Fig. 9), most probably from the Ediacaran and Cambrian metasedimentary rocks (Casquet and Galindo, 2004). However, Nd and Sr isotope ratios are different to those obtained from the Almansor diatexites, suggesting that they do not result from melting of the same type of source rock within the wide field defined by Casquet and Galindo (2004). The isotope composition of the two-mica leucogranite does not constitute a suitable felsic endmember for the mixing line defined by the other granitoid rocks of the area. Therefore, it seems that this peraluminous granite, despite its volumetric importance at Alto de São Bento had little geochemical interaction with more mafic magmas.

Low incompatible element contents, flat normalized REE patterns and strong negative Eu anomalies suggest that the two-mica leucogranites correspond to a magma produced either by: (1) low degree of partial melting in the presence of refractory plagioclase and accessory phases with high partition coefficients for hygromagmatophile trace elements, or by (2) a high degree of fractionation of an anatectic melt.

The presence of a plutonic suite with a calc-alkaline signature is consistent with an evolution of the studied area at an active continental margin during the Late Palaeozoic. This type of setting has already been proposed for the generation of granitoid rocks in other sectors of the OMZ (e.g. Castro et al., 1990; Moreno-Ventas et al., 1995; Castro et al., 1999b; Casquet and Galindo, 2004). Closer to the study area, there are also volcanic remnants of a magmatic arc, along the SW border of the Ossa–Morena Zone (Santos et al., 1987, 1990; Chichorro, 2006).

7.4. Different types of Variscan plutonism in the Évora high-grade metamorphic terrain

The three areas studied are all located within the same high-grade metamorphic terrain and seem to represent magmatic events with similar ages (as discussed above), but they exhibit very different mesoscopic features, in particular the presence or absence of a foliation. However, this contradiction may be only apparent, since, as stressed by several authors (Pe-Piper et al., 2002; Bea et al., 2004; Stålfors and Ehlers, 2005), variable importance of anisotropic structures/textures amongst intrusive bodies does not necessarily imply that they have very distinct chronological positions in relation to the regional deformation phases.

At Almansor and Alto de São Bento, granitoids show very different field relationships but they share some significant characteristics; they include lithologies with calc-alkaline fingerprints, which probably belong to a plutonic suite with major expression throughout the EHMT and represented by a wide compositional range (from gabbros to granites). There are also, in both areas, remnants from the anatexis of metasedimentary rocks, most likely from Série Negra. Those two areas may be regarded as corresponding to different sectors of a major structure (Fig. 10) similar to the model proposed by Stålfors and Ehlers (2005); Almansor is located within a shear zone through which melt batches (of more than one origin) ascended through the crust and, in some cases, crystallized into foliated rocks, due to magma flux controlled by the tectonic stress field. Alto de São Bento represents a higher crustal level, where granitoid bodies, fed by the shear zone, were emplaced as laterally spreading sub-horizontal sheets, where melt batches moved away from the zone of maximum tectonic stress.

The calc-alkaline signature, commonly found in the igneous rocks that occur in the studied region, indicates the existence of continental arc-type magmatism during the Lower Carboniferous at the SW border of the OMZ. This magmatism probably results from the subduction of oceanic lithosphere under the OMZ, during the Variscan orogeny, and subsequent genesis of mafic magmas in the supra-subduction mantle wedge. The ascent of mantle-derived magmas, revealed by several gabbroic intrusions in the OMZ, and consequent transfer of large amounts of heat to the crustal rocks, may be viewed as an important factor in promoting anatexis of Ediacaran Série Negra metasediments.

The Valverde area represents a more circumscribed process that is not easily reconciled with the evidence from the other two other areas. Granitoids, from Valverde, studied here are trondhjemites with geochemical features that could correspond to a highly differentiated calc-alkaline magma. However, they plot outside the mixing curve defined by other calc-alkaline lithologies occurring in the EHMT, showing that the genesis of Valverde granitoids is unique: (1) their parental magma was clearly different to the parental magmas of the dominant plutonic suite in the region; or (2) they belong to a mixing line with different endmembers; or (3) they represent an anatectic magma produced by melting of an orthogneiss, and not of metasediments. Whatever the correct answer is, the Valverde lithologies have a peculiar place in the framework of magmatic lithologies in the EHMT.

8. Conclusions

Variscan granitoid rocks from three different areas within the Évora High-Grade Metamorphic Terrain were studied with the aim of establishing the origin of the different magma compositions and recognizing the nature of mesoscopic structures, observed in some places, that is suggestive of migmatization processes.

The Valverde outcrop is still enigmatic and further studies are required. However the “migmatitic appearance” probably does not

represent an *in situ* melting event, since the two lithologies distinguished during field studies have very similar modal compositions and show no geochemical fractionation amongst them. As such, the mesoscopic relationships may, in fact, testify to processes of internal segregation of the same magma. This magma had a calc-alkaline signature, but, isotopically, it was distinct from the mixing trend defined by calc-alkaline rocks from other areas within EHMT. Therefore, the genesis of Valverde granitoids either involved different parental magmas (and/or endmember of mixing processes) or corresponds to the crystallization of a melt produced by anatexis of orthogneisses.

The conspicuous layered structure observed at Almansor, once again, rather than testifying to *in situ* anatexis of crustal rocks, corresponds probably to complex injection of several magmas formed by different processes – crustal anatexis, fractional crystallization of mantle derived melts and mingling/mixing – along an active shear zone. Diatexites should result from melting of metasedimentary rocks (Série Negra Ediacaran paragneisses and micaschists) and the range of chemical and modal compositions that they exhibit was probably caused by varying amounts of incorporated refractory material (mostly represented by biotite). Weakly foliated granitoids have a calc-alkaline signature and seem to derive from more mafic magmas, through processes involving differentiation by fractional crystallization, as well as hybridization with diatexitic magmas. Trondhjemitic veins are genetically related to the weakly foliated granitoids and should correspond to magmas resulting from a more advanced differentiation stage.

Alto de São Bento granitoids can be regarded as being linked, in a higher crustal level, to the Almansor structure. At Alto de São Bento, both anatectic (probably derived from partial melting of Série Negra metasedimentary rocks) and calc-alkaline magmas were emplaced mainly as sub-horizontal sheets. The Almansor outcrop can be viewed as the remain of a shear zone that operated as a pathway of melts upwards through the crust in the EHMT, whilst Alto de São Bento would correspond to the zone where magmas were trapped and forced to spread horizontally.

Acknowledgments

Research was supported by Centro de Geofísica de Évora and CHRONOTECT (POCTI/CTE-GIN/60043/2004) - FCT scientific project. The authors are indebted to Cristina Ribeiro for providing 3 samples and data from the Alto de S. Bento area and to Martim Chichorro for stimulating discussions. Pedro Madureira and José Mirão are thanked for invaluable assistance in the field. We would also like to thank António Castro, Edward Sawyer and Stefan Jung for their constructive and supportive comments which greatly improved the manuscript.

Appendix A. Analytical techniques

I. Major and trace elements analyses were performed at Activation Laboratories — ACTLABS (Canada) using the lithium metaborate/tetraborate fusion for ICP (Code 4B) and ICP-MS (Code 4B2). Samples are prepared and analysed in a batch system. Each batch contains a reagent blank, a certified reference material and 17% replicates. Samples are mixed with a flux of lithium metaborate and lithium tetraborate and fused in an induction furnace. The resulting melt is immediately poured into a solution of 5% nitric acid containing an internal standard, and mixed continuously until completely dissolved (~30 min). The samples were run for major and trace elements on a combination of simultaneous/sequential Thermo Jarrell-Ash ENVIRO II ICP. Calibration was performed using seven USGS and Canmet certified reference materials. One of the seven standards is used during the analysis for every group of samples. The sample solution prepared under Code 4B is spiked with internal standards to cover the entire mass range, and is further diluted to cover the entire mass range, is further diluted and is introduced into a Perkin Elmer SCIEX ELAN 6000 or 6100 ICP-MS using a proprietary (ACTLABS) sample introduction methodology.

II. Isotopic data were obtained from 14 samples from the three areas. The samples were dissolved with HF/HNO_3 in Teflon Parr acid digestion bombs at 200 °C. After evaporation of the final solution, the samples were dissolved with HCl (6 N) and dried down. The elements for analysis were purified using a conventional two-stage ion chromatography technique: (i) separation of Sr and REE elements in ion exchange column with AG8 50 W Bio-Rad cation exchange resin; (ii) purification of Nd from others lanthanide elements in columns with Ln Resin (ElChroM Technologies) cation exchange resin. All the reagents in the preparation of the samples were sub-boiling distilled, and the water was produced by a Milli-Q Element (Millipore) apparatus. The isotopic analysis were carried out at the Laboratório de Geologia Isotópica da Universidade de Aveiro (Portugal). Sr was loaded on a single Ta filament with H_3PO_4, whereas Nd was loaded on a Ta outer side filament with HCl, in a triple filament arrangement. Both elements were determined using a Multi-Collector Thermal Ionisation Mass Spectrometer (TIMS) VG Sector 54. Data were obtained at dynamic mode with peak measurements at 1–2 V for ^{88}Sr and 0.8–1.5 V for ^{144}Nd. Sr and Nd isotopic ratios were corrected for mass fractionation relative to $^{88}Sr/^{86}Sr = 0.1194$ and $^{146}Nd/^{144}Nd = 0.7219$. During this study, the SRM-987 standard gave an average value of $^{87}Sr/^{86}Sr = 0.710263(6)$ (N = 20; 95% c.l.) and $^{143}Nd/^{144}Nd = 0.512098(2)$ (N = 29; 95% c.l.) to JNdi-1 standard ($^{143}Nd/^{144}Nd$ data are normalized to La Jolla standard).

References

Antunes, A., 2006. Rochas Granitóides da Zona de Ossa Morena: Magmatismo, Geodinâmica e reconstituição geohistórica. Unpublished MSc thesis, Universidade de Aveiro, 181 pp.

Barbey, P., Bertrand, J., Angoua, S., Dautel, D., 1989. Petrology and U/Pb geochronology of the Telohat migmatites, Aleksod, Central Hoggar, Algeria. Contributions to Mineralogy and Petrology 101, 207–219.

Bea, F., 1996. Residence of REE, Y, Th and U in granites and crustal protoliths: implications for the chemistry of crustal melts. Journal of Petrology 37, 521–552.

Bea, F., Fershtater, G., Montero, P., Smirnov, V., Molina, J., 2004. Deformation-driven differentiation of granitic magma: the Stepninsk pluton of the Uralides, Russia. Lithos 81, 209–233.

Brown, M., 1973. Definition of metatexis, diatexis and migmatite. Proceedings of the Geologists' Association 84, 371–382.

Brown, M., 1994. The generation, segregation, ascent and emplacement of granite magma: the migmatite-to-crustally-derived connection in thickened orogens. Earth Science Reviews 36, 83–130.

Carbonell, R., Simancas, F., Juhlin, C., Pous, J., Pérez-Estaún, Gonzalez_Lodeiro, F., Muñoz, Heise, W., Ayarza, P., 2004. Geophysical evidence of a mantle derived intrusion in the SW Iberia. Geophysics Research Letters 31, L11601.

Carvalhosa, A., 1983. Esquema geológico do Maciço de Évora. Comunicações dos Serviços Geológicos de Portugal 69 (2), 201–208.

Carvalhosa, A., Zbyszewski, G., 1994. Carta Geológica de Portugal 1:50.000 - Notícia explicativa da folha 35-D, Montemor-o-Novo. Instituto Geológico e Mineiro. 86 pp.

Carvalhosa, A., Carvalho, A., Alves, C., Pina, H., 1969. Carta Geológica de Portugal na Escala 1: 50 000 - Notícia Explicativa da Folha 40-A, Évora. Serviços Geológicos de Portugal, Lisboa. 26 pp.

Casquet, C., Galindo, C., 2004. Magmatismo varisco y postvarisco en la Zona de Ossa–Morena. In: Vera, J.A. (Ed.), Geología de España. Sociedad Geológica de España, IGME, Madrid, pp. 194–198.

Castro, A., De La Rosa, J., 2002. Intrusive rocks of the Southern Iberian Massif. In: Gibbons, W., Moreno, M.T. (Eds.), The Geology of Spain. Geological Society, London, pp. 138–141.

Castro, A., Moreno-Ventas, I., De La Rosa, J., 1990. Microgranular enclaves as indicators of hybridization processes in granitoid rocks, Hercynian Belt, Spain. Geological Journal 25, 391–404.

Castro, A., Fernández, C., El-Hmidi, H., El-Biad, M., Díaz, M., De La Rosa, J., Stuart, F., 1999a. Age constraints to the relationships between magmatism, metamorphism and tectonism in the Aracena metamorphic belt, southern Spain. International Journal of Earth Science 88, 26–37.

Castro, A., Patiño Douce, A.E., Corretgé, L.G., de la Rosa, J., El-Biad, M., El-Hmidi, H., 1999b. Origin of peraluminous granites and granodiorites; Iberian massif, Spain: an experimental test of granite petrogenesis. Contributions to Mineralogy and Petrology 135, 255–276.

Chichorro, M., 2006. A Evolução Tectónica da Zona de Cisalhamento de Montemor-o-Novo (Sudoeste da Zona de Ossa Morena – Área de Santiago do Escoural – Cabrela). Unpublished PhD thesis, Universidade de Évora, 521 pp.

Chichorro, M., Pereira, M.F., Díaz-Azpiroz, Williams, I.S., Fernández, C., Pin, C., Silva, J.B., 2008. Cambrian ensialic rift related magmatism in the Ossa–Morena Zone (Évora-

Aracena metamorphic belt, SW Iberain Massif): Sm–Nd isotopes and SHRIMP zircon U–Th–Pb geochronology. Tectonophysics 461 (1–4), 91–113.
Clarke, D., 1992. Granitoid Rocks. Chapman and Hall, New York. 283 pp.
Cordani, U., Nutman, A., Andrade, A., Santos, J., Azevedo, M., Mendes, M., Pinto, M., 2006. New U–Pb SHRIMP zircon ages for pre-variscan orthogneisses from Portugal and their bearing on the evolution of the Ossa–Morena Tectonic Zone. Anais da Academia Brasileira das Ciências 78 (1), 133–149.
De la Roche, H., Leterrier, J., Grandclaude, P., Marchal, M., 1980. A classification of volcanic and plutonic rocks using R1–R2 diagrams and major element analyses — its relationships and current nomenclature. Chemical Geology 29, 183–210.
Defant, M., Drummond, M., 1990. Derivation of some modern arc magmas by melting of young subducted lithosphere. Nature 347, 662–665.
Díaz Azpiroz, M., Castro, A., Fernández, C., López, S., Fernández Caliani, J., Moreno-Ventas, I., 2004. The contact between the Ossa–Morena and the South Portuguese zones. Characteristics and significance of the Aracena metamorphic belt, in its central sector between Aroche and Aracena (Huelva). Journal of Iberian Geology 30, 23–51.
El-Biad, M., 2000. Generación de Granitoides en Ambientes Geológicamente Contrastados del Macizo Ibérico. Limitaciones Experimentales entre 2 y 15 kbar. PhD thesis, Universidad de Huelva.
Fujimaki, H., 1986. Partition coefficients of Hf, Zr and REE between zircon, apatite and liquid. Contributions to Mineralogy and Petrology 94, 42–45.
Hensen, B.J., Osanai, Y., 1994. Experimental study of dehydration melting of F-bearing biotite in model pelitic compositions. Mineralogical Magazine 58A, 410–411.
Holden, P., Halliday, A., Stephens, W., 1987. Neodymium and strontium isotope content of microdiorite enclaves points to mantle input to granitoid production. Nature 330, 53–56.
Jacobsen, S.B., Wasserburg, G.J., 1980. Sm–Nd isotopic evolution of chondrites. Earth and Planetary Science Letters 50, 139–155.
Johannes, W., Holtz, F., Möller, P., 1995. REE distribution in some layered migmatites: constraints on their petrogenesis. Lithos 35, 139–152.
Jung, S., Hoernes, S., Masberg, P., Hoffer, E., 1999. The petrogenesis of some migmatites and granites (Central Damara Orogen, Namibia): evidence for disequilibrium melting, wall-rock contamination and crystal fractionation. Journal of Petrology 40, 1241–1269.
Kretz, R., 1983. Symbols for rock-forming minerals. American Mineralogist 68, 277–279.
Lesher, C., 1990. Decoupling of chemical and isotopic exchange during magma mixing. Nature 344, 235–237.
Lucas, S.B., St-Onge, M.R., 1995. Syn-tectonic magmatism and the development of compositional layering, Ungava Orogen (northern Quebec, Canada). Journal of Structural Geology 17, 475–491.
Mehnert, K.R., 1968. Migmatites and the Origin of Granitic Rocks. Elsevier, Amsterdam. 393 pp.
Miller, C., 1985. Are strongly peraluminous magmas derived from pelitic sedimentary sources? Journal of Geology 93, 673–689.
Miller, C.F., Watson, M.E., Harrison, T.M., 1988. Perspective on the source, segregation and transport of granitoid magmas. Royal Society of Edinburgh Transactions 79, 135–156.
Miller, C., McDowell, S., Mapes, R., 2003. Hot and cold granites? Implications of zircon saturation temperatures and preservation of inheritance. Geology 31, 529–532.
Milord, I., Sawyer, E., 2003. Schlieren formation in diatexite migmatite: examples from the St. Malo migmatite terrane, France. Journal of Metamorphic Geology 21, 347–362.
Milord, I., Sawyer, E., Brown, M., 2001. Formation of diatexite migmatite and granite magma during anatexis of semi-pelitic metasedimentary rocks: an example from St. Malo, France. Journal of Petrology 42, 487–505.
Moita, P., 2007. Granitóides no SW da Zona de Ossa Morena (Montemor-o-Novo – Évora): Petrogénese e Processos Geodinâmicos. Unpublished PhD thesis, Universidade de Évora, 351 pp.
Moita, P., Pereira, M.F., Santos, J., 2005a. Tonalites from the Hospitais massif (Ossa–Morena Zone, SW Iberian Massif, Portugal). I: geological setting and petrography. Geogaceta 37, 51–54.
Moita, P., Santos, J., Pereira, M.F., 2005b. Tonalites from the Hospitais massif (Ossa–Morena Zone, SW Iberian Massif, Portugal). II: geochemistry and petrogenesis. Geogaceta 37, 55–58.
Moita, P., Santos, J.F., Pereira, M., 2005c. Dados geocronológicos de rochas intrusivas sintectónicas no Maciço dos Hospitais (Montemor-o-Novo, Zona de Ossa Morena). Actas da XIV Semana de Geoquímica / VIII Congresso de Geoquímica dos Países de Língua Portuguesa 2, 471–474.
Moreno-Ventas, I., Rogers, G., Castro, A., 1995. The role of hybridization in the genesis of Hercynian granitoids in the Gredos Massif, Spain: inferences from Sr, Nd isotopes. Contributions to Mineralogy Petrology 120, 137–149.
Myers, J.S., 1978. Formation of banded gneisses by deformation of igneous rocks. Precambrian Research 6, 43–64.
O'Connor, J.T., 1965. A classification for quartz-rich igneous rock based on feldspar ratios. United States Geological Survey Professional Paper 525, B79–B84.
Oliveira, J., Oliveira, V., Piçarra, J., 1991. Traços gerais da evolução tectono-estratigráfica da Zona de Ossa Morena. Comunicações dos Serviços Geológicos de Portugal 77, 3–26.
Passchier, C.W., Myers, J.S., Kröner, A., 1990. Field Geology of High-grade Gneiss Terrains. Springer-Verlag, Heidelberg. 147 pp.
Passchier, C.W., Trouw, R.A.J., 1998. Microtectonics. Springer 289 pp.
Patiño Douce, A.E., 1999. What do experiments tell us about the relative contributions of crust and mantle to the origin of granitic magmas? In: Castro, A., Fernández, C., Vigneresse, J. (Eds.), Understanding granites. Integrating New and Classical Techniques. Geological Society of London, Special Publication, vol. 168, pp. 55–75.
Patiño Douce, A.E., Harris, N., 1998. Experimental constraints on Himalayan anatexis. Journal of Petrology 4, 689–710.
Patiño Douce, A.E., Castro, A., El-Biad, M., 1997. Thermal evolution and tectonic implications of spinel-cordierite granulites from the Aracena Metamorphic Belt; Southwest Spain. GAC/MAC Annual Meeting 22, A113.
Pawley, M.J., Collins, W.J., Van Kranendonk, M.J., 2002. Origin of fine-scale sheeted granites by incremental injection of magma into active shear zones: examples from the Pilbara Craton, NW Australia. Lithos 61, 127–139.
Pe-Piper, G., Piper, D.J.W., Matarangas, D., 2002. Regional implications of geochemistry and style of emplacement of Miocene I-type diorite and granite, Delos, Cyclades, Greece. Lithos 60, 47–66.
Pereira, M.F., Silva, J.B., 2002. The geometry and kinematics of enclaves in sheared migmatites from the Évora Massif, Ossa–Morena Zone (Portugal). Geogaceta 31, 193–196.
Pereira, M.F., Lúcio, P.S., 2007. Understanding geological data distribution and orientation via correspondence analysis. Mathematical Geology 39, 673–695.
Pereira, M.F., Silva, J.B., Chichorro, M., 2003. Internal structure of the Évora high-grade metamorphic terrains and the Montemor-o-Novo Shear Zone (Ossa–Morena Zone, Portugal). Geogaceta 33, 71–74.
Pereira, M.F., Chichorro, M., Silva, J.B., 2006a. Variscan extensional tectonics in the Évora Massif (Ossa Morena Zone): the Valverde cross section. Livro de Resumos do VII Congresso Nacional de Geologia I, 43–46.
Pereira, M., Chichorro, M., Linneman, U., Eguíluz, L., Silva, J., 2006b. Inherited arc signature in Ediacaran and Early Cambrian basins of the Ossa–Morena Zone (Iberian Massif, Portugal): paleogeographic link with European and North African Cadomian correlatives. Precambrian Research 144, 297–315.
Pereira, M., Medina, J., Chichorro, M., Linnemann, U., 2006c. Preliminary Rb–Sr and Sm–Nd isotope geochemistry on Ediacaran and Early Cambrian sediments from the Ossa–Morena Zone (Portugal). Livro de Resumos do VII Congresso Nacional de Geologia I, 213–215.
Pereira, M., Silva, J., Chichorro, M., Moita, P., Santos, J., Apraíz, A., Ribeiro, C., 2007. Crustal growth and deformational processes in the northern Gondwana margin: constraints from the Évora Massif (Ossa–Morena Zone, SW Iberia, Portugal). In: Linnemann, U., Nance, R.D., Kraft, P., Zulauf, G. (Eds.), The Evolution of the Rheic Ocean; From Avalonian- Cadomian Active Margin to Alleghenian-Variscan Collision. Geological Society of America, Special Paper, vol. 423, pp. 333–358.
Ribeiro, A., 1983. Relações entre formações do Devónico superior e o Maciço de Évora na região de Cabrela (Vendas Novas). Comunicações dos Serviços Geológicos de Portugal 69, 267–282.
Ribeiro, C., 2006. Cartografia de rochas ígneas: Análise da Orientação Preferencial de Fenocristais de Feldspato para Caracterização do Fluxo Magmático nos Granitóides Porfiróides do Alto de São Bento (Maciço de Évora, Zona de Ossa Morena). Unpublished MSc thesis, Universidade de Évora, 160 pp.
Robin, P.Y., 1979. Theory of metamorphic segregation and related processes. Geochimica et Cosmohimica Acta 43, 1587–1600.
Rudnick, S., Gao, W., 2003. The composition of the continental crust. In: Holland, H., Turekian, K. (Eds.), Treatise on Geochemistry, 3. Elsevier, New York, pp. 1–64.
Santos, J., Mata, J., Gonçalves, F., Munhá, J., 1987. Contribuição para o conhecimento geológico-petrológico da região de Santa Susana: o complexo vulcano-sedimentar da Toca da Moura. Comunicações dos Serviços Geológicos Portugal 73, 29–48.
Santos, J., Andrade, A., Munhá, J., 1990. Magmatismo orogénico varisco no limite meridional da Zona de Ossa–Morena. Comunicações dos Serviços Geológicos Portugal 76, 91–124.
Sawyer, E.W., 1996. Melt segregation and magma flow in migmatites: implications for the generation of granite magmas. Royal Society of Edinburgh Transactions Earth Sciences 87, 85–94.
Sawyer, E.W., 2000. Grain-scale and outcrop-scale distribution and movement of melt in a crystallizing granite. Royal Society of Edinburgh Transactions Earth Sciences 91, 73–85.
Sawyer, E.W., 2001. Melt segregation in the continental crust: distribution and movement of melt in anatectic rocks. Journal of Metamorphic Geology 19, 291–309.
Sawyer, E.W., 2008. Working with migmatites: nomenclature for the constituent parts. Mineralogical Association of Canada Short Course 38, 1–28.
Sawyer, E.W., Barnes, S.J., 1988. Temporal and compositional differences between subsolidus and anatectic migmatite leucosomes from the Quetico metasedimentary belt, Canada. Journal of Metamorphic Geology 6, 437–450.
Shand, S.J., 1947. Eruptive Rocks. Their Genesis, Composition, Classification, and their Relation to Ore-deposits. J. Wiley and Sons, New York. 488 pp.
Shelley, D., 1993. Igneous and Metamorphic rocks under the microscope: Classification, Textures, Microstructures and Mineral Preferred Orientations. Chapman and Hall, New York. 496 pp.
Sheppard, S., Occhipinti, S., Tyler, I., 2003. The relationship between tectonism and composition of granitoid magmas, Yarlarweelor Gneiss Complex, Western Australia. Lithos 66, 133–154.
Stålfors, T., Ehlers, C., 2005. Emplacement mechanisms of late-orogenic granites: structural and geochemical evidence from southern Finland. International Journal of Earth Sciences 95 (4), 557–568.
Sun, S., McDonough, W., 1989. Chemical and isotopic systematics of oceanic basalts: implications for mantle composition and processes. In: Saunders, A., Norry, M. (Eds.), Magmatism in Ocean Basins. Geological Society London Special Publication, vol. 42, pp. 313–345.
Vernon, R., 2000. Review of microstructural evidence of magmatic and solid and solid-state flow. Electronic Geosciences 5 (2).
Watson, E., Harrison, T., 1983. Zircon saturation revisited: temperature and composition effects in a variety of crustal magma types. Earth Planetary Science Letters 64, 295–304.
Weinberg, R.F., 2006. Melt segregation structures in granitic plutons. Geology 34, 305–308.
Weinberg, R.F., Sial, A.N., Pessoa, R.R., 2001. Magma flow within the Tavares Pluton, NE Brazil: compositional and thermal convection. Geological Society of America Bulletin 113, 508–520.
Zeng, L., Saleeby, J., Asimov, P., 2005. Nd isotope disequilibrium during crustal anatexis: a record from the Goat Ranch migmatite complex, southern Sierra Nevada batholith, California. Geology 33, 53–56.